Universiteit Utrecht

Opleiding Natuur- en Sterrenkunde

Effect of the Geometry of an Yttrium Iron Garnet Film on the Spin-Wave Dispersion Relation

Bachelor Thesis

Mithuss Tharmalingam

Supervisors:

Ir. P. M. Gunnink
Institute for Theoretical Physics at Utrecht University

Prof. Dr. R. A. Duine
Institute for Theoretical Physics at Utrecht University

January 18, 2021

Abstract

In the last couple of years spintronics gained much attention as a research area. The reason for this is that spintronics signal processing devices could replace conventional electronic devices. As of lately, spin waves carrying spin currents in magnetic insulators like yttrium iron garnet (YIG) have been studied. For example, there has been research on a YIG film with an external magnetic field and motivated by the results we will verify it. Furthermore we will consider holes in the film to obtain new results. In our thesis we will use the Holstein-Primakoff transformation to find the dispersion relation of a Hamiltonian, considering the exchange and dipole-dipole interaction. We will do this via numerical simulations. To lower the computational time we will use the Ewald summation for the dipole-dipole interaction. Furthermore, we shall give a motivation on why the Ewald summation gives reliable results and why it lowers the computational time. Our results show that there are bandgaps in our dispersion relation, which were also found experimentally in Wang *et al.* If we neglect the exchange interaction we found a similar shape as well. The results we obtained could be used to develop ways to control spin waves in magnetic insulators.

Contents

1 Introduction

As time progresses computers become more important in our lives. One problem that computers have, is that they need a lot of power and the solution to this problem might lie in the field of spintronics [1]. Instead of using electrons, one could use spin waves as information carriers [2], which could solve the power problem. The reason why is that there will not be any Joule heating as a result of moving electrons. To understand what spin waves are, we consider a lattice consisting of magnetic moments. If we apply a strong enough external magnetic field, all these magnetic moments will align along the direction of the magnetic field. A disturbance of one of these magnetic moments will cause a disturbance to its neighbours, because the spins are linked to each other due to the exchange and dipole-dipole interaction. As a result a wave propagates through the lattice which is visualized in Figure 1. This wave is called a spin wave.

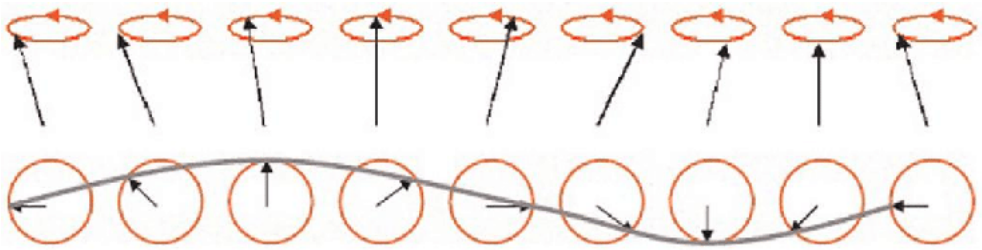

Figure 1: *A spin wave from two perspectives. The top one shows the front view of a spin wave and the bottom one shows the perspective from above. The arrows represent the spin vectors and the drawn wave goes through the end of those spin vectors. Copyright: Ivan S. Maksymov, Mikhail Kostylev (2015) [3].*

In our research we consider the easily tunable YIG film as our lattice. Another reason why we consider YIG is the fact that it has an almost perfect cubic symmetry [4]. In this thesis we investigate the role of the geometry of a YIG film on the dispersion relation of the spin waves. We will do this by comparing a lattice without holes to a lattice with holes. The comparison shall be done using numerical simulations. The reason why we add holes is because we expect bandgaps comparable to the electronic band structure of a solid. The theory on bandgaps in the electronic band structure of a solid is important to understand solid state devices such as transistors. In our case the bandgaps might be used to manipulate the spin wave transport in the future. More information on this can be found in Chumak *et al.* [5]. The dispersion relation of spin waves in a YIG film without holes has already been determined by Kreisel *et al.* [6]. We will study their method and adapt it to the case of a YIG film with holes. We expect to find bandgaps in our dispersion relation which have been observed experimentally by Wang *et al.* [7]. We will show how to reproduce this in Chapter 3. We begin this thesis with studying the methods of Ref. [6] in Chapter 2. Moreover, will adjust their theory to fit in the new situation of a lattice with holes. We end this chapter on how to obtain the dispersion relation. To lower the computation time of finding the dispersion relation we use the Ewald summation. In Chapter 3 we show that the Ewald summation indeed lowers the computation time and additionally we present the dispersion relation of both a YIG film with and without holes. Also, we consider the dispersion relation where we neglect the exchange interaction. The results will be discussed in Chapter 4 and we we will draw conclusions in the final chapter.

2 Theory

As mentioned in the introduction we intend to find the dispersion relation of spin waves on a normal cubic lattice and that of a lattice with holes. Before we can do that we shall discuss some theory about the Hamiltonian in both situations. In the first section, which is about the Hamiltonian in the case of a lattice without holes, we will mainly follow the work by Kreisel *et al.* [6]. What we will do first is determine the Hamiltonian and apply the Holstein-Primakoff transformation. Thereafter we apply a Fourier transformation such that we can numerically diagonalize the Hamiltonian. In the second section we will do the same but in the situation of a lattice with holes.

2.1 Hamiltonian

Let us first describe the situation. We consider a cubic lattice made out of YIG with a lattice constant equal to $a = 12.376$ Å [4]. Our lattice has an infinite length, a width w and a height $d = Na$ as we can see in Figure 2. Furthermore, we add an external magnetic field $\mathbf{H}_e$ along the z-direction.

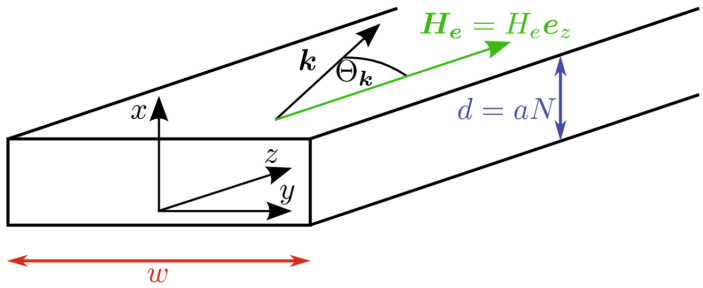

Figure 2: *Schematic visualisation of the system. Here w is the width and $d = aN$ the height. The magnetic field $\boldsymbol{H}_e$ is in the z direction and the wavevector k is in the y, z-plane. In our research we will only consider the wavevector to be in the z-direction. Copyright: Kreisel et al. (2009) [6].*

As discussed in Ref. [6] we can describe this situation as a quantum Heisenberg ferromagnet with effective spin S where we consider the exchange energy, the Zeeman energy and the energy as the result of the dipole-dipole interactions. The corresponding Hamiltonian is then given by:

$$\hat{H} = -\frac{1}{2}\sum_{ij} J_{ij}\mathbf{S}_i \cdot \mathbf{S}_j - \mu\mathbf{H}_e \cdot \sum_i \mathbf{S}_i - \frac{1}{2}\sum_{ij,i\neq j} \frac{\mu^2}{|\mathbf{R}_{ij}|^3}\left[3(\mathbf{S}_i \cdot \hat{\mathbf{R}}_{ij})(\mathbf{S}_j \cdot \hat{\mathbf{R}}_{ij}) - \mathbf{S}_i \cdot \mathbf{S}_j\right], \tag{1}$$

where $\sum_{ij}$ indicates the double sum over the lattice sites. Here J_{ij} is the exchange energy which is equal to J if i and j are nearest neighbours and equal to 0 otherwise. Furthermore, $\mu = g\mu_B$, where g is the effective g-factor and μ_B the Bohr magneton. Finally, we define $\mathbf{R}_i$ to be the position vector of site i. Then $\mathbf{R}_{ij}$ is the difference vector $\mathbf{R}_i - \mathbf{R}_j$ and $\hat{\mathbf{R}}_{ij}$ is the unit vector of $\mathbf{R}_{ij}$.

Let us define $D_{ij}^{\alpha\beta}$ in the following way,

$$D_{ij}^{\alpha\beta} = (1-\delta_{ij})\frac{\mu^2}{|\mathbf{R}_{ij}|^3}\left[3\hat{R}_{ij}^{\alpha}\hat{R}_{ij}^{\beta} - \delta^{\alpha\beta}\right],$$

where α and β are the x, y or z-direction. Then we write our Hamiltonian as

$$\hat{H} = -\frac{1}{2}\sum_{ij}\sum_{\alpha\beta}\left[J_{ij}\delta^{\alpha\beta} + D_{ij}^{\alpha\beta}\right] S_i^{\alpha} S_j^{\beta} - h\sum_i S_i^z, \tag{2}$$

where $h = \mu|\mathbf{H}_e|$, which is the Zeeman energy. We use the Holstein-Primakoff transformation to replace the spin operator with other operators which we will specify later. According to Ref. [6] the effective spin is so large that we only need to consider the Hamiltonian up to quadratic order in the new operators. To apply the Holstein-Primakoff transformation we introduce, as in Ref. [8], S_i^+ and S_i^- such that

$$S_i^x = \frac{S_i^+ + S_i^-}{2},$$

and

$$S_i^y = \frac{S_i^+ - S_i^-}{2i}.$$

Applying the Holstein-Primakoff transformation gives,

$$S_i^+ = \sqrt{2S}\,\sqrt{1-\frac{a_i^\dagger a_i}{2S}}\;a_i;$$
$$S_i^- = \sqrt{2S}\;a_i^\dagger\,\sqrt{1-\frac{a_i^\dagger a_i}{2S}},$$

where a_i and $a_i^\dagger$ are bosonic creation and annihilation operators with the property that

$$[a_i, a_i^\dagger] = 1.$$

Note that we take the square root of operators, so we need a Taylor approximation, which we will do later. Using

$$[S_i^+, S_j^-] = 2S_i^z\delta_{ij},$$

we can determine S_i^z in the following way,

$$\begin{aligned}
S_i^z &= \frac{1}{2}[S_i^+, S_i^-] \\
&= \frac{1}{2}\left(\sqrt{2S}\,\sqrt{1-\frac{a_i^\dagger a_i}{2S}}\;a_i\cdot\sqrt{2S}\;a_i^\dagger\,\sqrt{1-\frac{a_i^\dagger a_i}{2S}} - \sqrt{2S}\;a_i^\dagger\,\sqrt{1-\frac{a_i^\dagger a_i}{2S}}\cdot\sqrt{2S}\,\sqrt{1-\frac{a_i^\dagger a_i}{2S}}\;a_i\right) \\
&= S\left(\sqrt{1-\frac{a_i^\dagger a_i}{2S}}\;a_i a_i^\dagger\sqrt{1-\frac{a_i^\dagger a_i}{2S}} - a_i^\dagger\left(1-\frac{a_i^\dagger a_i}{2S}\right)a_i\right) \\
&= S\left(\sqrt{1-\frac{a_i^\dagger a_i}{2S}}\;(1+a_i^\dagger a_i)\sqrt{1-\frac{a_i^\dagger a_i}{2S}} - a_i^\dagger a_i + \frac{a_i^\dagger a_i^\dagger a_i a_i}{2S}\right) \\
&= S\left(1-\frac{a_i^\dagger a_i}{2S} + a_i^\dagger a_i - \frac{a_i^\dagger a_i a_i^\dagger a_i}{2S} - a_i^\dagger a_i + \frac{a_i^\dagger a_i^\dagger a_i a_i}{2S}\right) \\
&= S\left(1-\frac{a_i^\dagger a_i}{2S} + a_i^\dagger a_i - \frac{a_i^\dagger a_i a_i^\dagger a_i}{2S} - a_i^\dagger a_i + \frac{a_i^\dagger(-1+a_i a_i^\dagger)a_i}{2S}\right) \\
&= S\left(1-\frac{a_i^\dagger a_i}{S}\right) \\
&= S - a_i^\dagger a_i.
\end{aligned}$$

For the effective spin we have $S \approx 14.2$ [6]. So, we can approximate S_i^+ and S_i^- by a first order Taylor approximation which results in

$$S_i^+ = \sqrt{2S}a_i;$$
$$S_i^- = \sqrt{2S}a_i^\dagger,$$

which leads to

$$S_i^x = \frac{\sqrt{2S}a_i + \sqrt{2S}a_i^\dagger}{2};$$
$$S_i^y = \frac{\sqrt{2S}a_i - \sqrt{2S}a_i^\dagger}{2i}.$$

Then we can write our Hamiltonian in the following way,

$$\hat{H} = \sum_n^\infty \hat{H}_n,$$

where $\hat{H}_n$ are the terms which are of n-th order in bosonic operators. Because of the fact that S is relatively large, we may neglect terms equal and larger than $n = 3$. The linear contribution $\hat{H}_1$ vanishes in the ground

state, such that we only need to focus on $\hat{H}_2$ to find the dispersion relation. We write the quadratic term as

$$\hat{H}_2 = \sum_{ij} \left[A_{ij} a_i^\dagger a_j + \frac{B_{ij}}{2} a_i a_j + \frac{B_{ij}^*}{2} a_i^\dagger a_j^\dagger \right] \tag{3}$$

from equation (2). Here we have

$$\begin{aligned} A_{ij} = {} & \delta_{ij} h + S(\delta_{ij} \sum_n J_{in} - J_{ij}) \\ & + S \left[\delta_{ij} \sum_n D_{in}^{zz} - \frac{D_{ij}^{xx} + D_{ij}^{yy}}{2} \right] \end{aligned}$$

and

$$B_{ij} = -\frac{S}{2} \left[D_{ij}^{xx} - 2iD_{ij}^{xy} - D_{ij}^{yy} \right],$$

which are called the amplitude factors. To derive equation (3) we start with equation (2) and apply the Holstein-Primakoff transformation. For that we determine $S_i^\alpha S_j^\beta$ for only the α and β which contribute to the quadratic part of the Hamiltonian. Note that S_i^x and S_i^y are linear in a_i and $a_i^\dagger$ and that S_i^z has a constant and a quadratic term. We then see that we only need to calculate terms with $S_i^x S_j^x$, $S_i^x S_j^y$, $S_i^y S_j^x$, $S_i^y S_j^y$ and $S_i^z S_j^z$, which are given below.

$$\begin{aligned}
-\frac{1}{2} \sum_{ij} \left[J_{ij} \delta^{xx} + D_{ij}^{xx} \right] S_i^x S_j^x &= \sum_{ij} -\frac{S}{4} \left[J_{ij} + D_{ij}^{xx} \right] \left(a_i a_j + a_i^\dagger a_j + a_i a_j^\dagger + a_i^\dagger a_j^\dagger \right) \\
&= \sum_{ij} -\frac{S}{2} \left[J_{ij} + D_{ij}^{xx} \right] a_i^\dagger a_j + \sum_{ij} -\frac{S}{4} \left[J_{ij} + D_{ij}^{xx} \right] \left(a_i a_j + a_i^\dagger a_j^\dagger \right); \\
-\frac{1}{2} \sum_{ij} \left[J_{ij} \delta^{yy} + D_{ij}^{xx} \right] S_i^y S_j^y &= \sum_{ij} -\frac{S}{4} \left[J_{ij} + D_{ij}^{yy} \right] \left(-a_i a_j + a_i^\dagger a_j + a_i a_j^\dagger - a_i^\dagger a_j^\dagger \right) \\
&= \sum_{ij} -\frac{S}{2} \left[J_{ij} + D_{ij}^{yy} \right] a_i^\dagger a_j + \sum_{ij} \frac{S}{4} \left[J_{ij} + D_{ij}^{yy} \right] \left(a_i a_j + a_i^\dagger a_j^\dagger \right); \\
-\frac{1}{2} \sum_{ij} \left[J_{ij} \delta^{xy} + D_{ij}^{xy} \right] S_i^x S_j^y &= \sum_{ij} -\frac{Si}{4} D_{ij}^{xy} \left(-a_i a_j - a_i^\dagger a_j + a_i a_j^\dagger + a_i^\dagger a_j^\dagger \right); \\
-\frac{1}{2} \sum_{ij} \left[J_{ij} \delta^{yx} + D_{ij}^{yx} \right] S_i^y S_j^x &= \sum_{ij} -\frac{Si}{4} D_{ij}^{yx} \left(-a_i a_j + a_i^\dagger a_j - a_i a_j^\dagger + a_i^\dagger a_j^\dagger \right) \\
&= \sum_{ij} -\frac{Si}{4} D_{ij}^{xy} \left(-a_i a_j + a_i^\dagger a_j - a_i a_j^\dagger + a_i^\dagger a_j^\dagger \right); \\
-\frac{1}{2} \sum_{ij} \left[J_{ij} \delta^{zz} + D_{ij}^{zz} \right] S_i^z S_j^z &= -\frac{1}{2} \sum_{ij} \left[J_{ij} \delta^{zz} + D_{ij}^{zz} \right] \left(S^2 - S a_i^\dagger a_i - S a_j^\dagger a_j + a_i^\dagger a_i a_j^\dagger a_j \right) \\
&= \sum_{ij} \frac{S}{2} \left[J_{ij} + D_{ij}^{zz} \right] (a_i^\dagger a_i + a_j^\dagger a_j) \\
&= \sum_{ij} S \left[J_{ij} + D_{ij}^{zz} \right] a_i^\dagger a_i \\
&= \sum_{in} S \left[J_{in} + D_{in}^{zz} \right] a_i^\dagger a_i \\
&= \sum_{ijn} S \delta_{ij} \left[J_{in} + D_{in}^{zz} \right] a_i^\dagger a_j,
\end{aligned}$$

where where we have neglected all constant and linear terms. Furthermore, we have

$$\begin{aligned} h \sum_i S_i^z &= h \sum_i (S - a_i^\dagger a_i) \\ &= h \sum_{ij} \delta_{ij} (S - a_i^\dagger a_i). \end{aligned}$$

Adding these terms to each other result in equation (3). Let our attention go back to the lattice again. We want to take w so large, that it is practically infinite with respect to the height N. We do this so that our lattice becomes basically invariant under translations in the y and z direction. To simplify the situation we may then perform a Fourier transformation. Our Hamiltonian then becomes

$$\hat{H}_2 = \sum_{\mathbf{k}} \sum_{x_i,x_j} \left[A_{\mathbf{k}}(x_{ij}) a^\dagger_{\mathbf{k}}(x_i) a_{\mathbf{k}}(x_j) + \frac{B_{\mathbf{k}}(x_{ij})}{2} a_{\mathbf{k}}(x_i) a_{-\mathbf{k}}(x_j) + \frac{B^*_{\mathbf{k}}(x_{ij})}{2} a^\dagger_{\mathbf{k}}(x_i) a^\dagger_{-\mathbf{k}}(x_j) \right], \tag{4}$$

where the Fourier transform of the creation and annihalation operators $a_{\mathbf{k}}(x_i)$ and $a^\dagger_{\mathbf{k}}(x_i)$ satisfy

$$a_i = \frac{1}{\sqrt{N_y N_z}} \sum_{\mathbf{k}} e^{i\mathbf{k}\cdot\mathbf{r}_i} a_{\mathbf{k}}(x_i);$$
$$a^\dagger_i = \frac{1}{\sqrt{N_y N_z}} \sum_{\mathbf{k}} e^{-i\mathbf{k}\cdot\mathbf{r}_i} a^\dagger_{\mathbf{k}}(x_i).$$

In equation (4) we have

$$A_{\mathbf{k}}(x_{ij}) = \sum_{\mathbf{r}} e^{-i\mathbf{k}\cdot\mathbf{r}} A^{\mathbf{r}0}_{ij},$$

where the lower indices in $A^{\mathbf{r}\mathbf{0}}_{ij}$ indicate the layers and the upper indices indicate the position within the layer. Here $\mathbf{r}$ is the position in layer i and $\mathbf{0}$ is the position in layer j. The expression $A_{\mathbf{k}}(x_{ij})$ is, in fact, the Fourier transform of $A^{\mathbf{r}0}_{ij}$. We can write $A^{\mathbf{r}0}_{ij}$ as

$$\begin{aligned}
A_{\mathbf{k}}(x_{ij}) = \sum_{\mathbf{r}} e^{-i\mathbf{k}\cdot\mathbf{r}} \Bigg[& \delta^{\mathbf{r}0}_{ij} h + S\delta^{\mathbf{r}0}_{ij} \sum_{\mathbf{r}',n} J^{\mathbf{r}\mathbf{r}'}_{in} - S J^{\mathbf{r}0}_{ij} \\
& + S\delta^{\mathbf{r}0}_{ij} \sum_{\mathbf{r}',n} D^{zz,\mathbf{r}\mathbf{r}'}_{in} - \frac{S}{2} \left(D^{xx,\mathbf{r}0}_{ij} + D^{yy,\mathbf{r}0}_{ij} \right) \Bigg] \\
= \delta_{ij} h + S\delta_{ij} & \sum_{\mathbf{r}',n} J^{\mathbf{r}'0}_{in} - S \sum_{\mathbf{r}} e^{-i\mathbf{k}\cdot\mathbf{r}} J^{\mathbf{r}0}_{ij} \\
& + S\delta_{ij} \sum_{\mathbf{r}',n} D^{zz,\mathbf{r}'0}_{in} - \frac{S}{2} \sum_{\mathbf{r}} e^{-i\mathbf{k}\cdot\mathbf{r}} \left(D^{xx,\mathbf{r}0}_{ij} + D^{xx,\mathbf{r}0}_{ij} \right) \\
= \delta_{ij} h + S\delta_{ij} & J \left(6 - \delta_{1j} - \delta_{Nj}\right) - SJ \left[\delta_{ij} \left(e^{-k_y a} + e^{ik_y a} + e^{-k_z a} + e^{ik_z a} \right) + \delta_{ij+1} + \delta_{ij-1} \right] \\
& + S\delta_{ij} \sum_{n} D^{zz}_0(x_{in}) - \frac{S}{2} \left[D^{xx}_{\mathbf{k}}(x_{ij}) + D^{yy}_{\mathbf{k}}(x_{ij}) \right] \\
= SJ_{\mathbf{k}}(x_{ij}) & + \delta_{ij} \left[h + S \sum_{n} D^{zz}_0(x_{in}) \right] + \frac{S}{2} \left[D^{xx}_{\mathbf{k}}(x_{ij}) + D^{yy}_{\mathbf{k}}(x_{ij}) \right],
\end{aligned}$$

where

$$J_{\mathbf{k}}(x_{ij}) = J[\delta_{ij}\{6 - \delta_{1j} - \delta_{Nj} - 2(\cos(k_y a) + \cos(k_z a))\} - \delta_{ij+1} - \delta_{ij-1}],$$

which we will call the exchange matrx. Before we continue we shall derive equation (4). We start with equation (3) and apply the Fourier transformation of the creation and annihilation opperator. We get

$$\begin{aligned}
\hat{H}_2 = \frac{1}{N_y N_z} \sum_{ij} \sum_{\mathbf{k}\mathbf{k}'} \Bigg[& A_{ij} e^{-i\mathbf{k}\cdot\mathbf{r}_i} e^{i\mathbf{k}'\cdot\mathbf{r}_j} a^\dagger_{\mathbf{k}}(x_i) a_{\mathbf{k}'}(x_j) \\
& + \frac{B_{ij}}{2} e^{i\mathbf{k}\cdot\mathbf{r}_i} e^{-i\mathbf{k}'\cdot\mathbf{r}_j} a_{\mathbf{k}}(x_i) a_{-\mathbf{k}'}(x_j) + \frac{B^*_{ij}}{2} e^{-i\mathbf{k}\cdot\mathbf{r}_i} e^{i\mathbf{k}'\cdot\mathbf{r}_j} a^\dagger_{\mathbf{k}}(x_i) a^\dagger_{-\mathbf{k}'}(x_j) \Bigg] \\
= \frac{1}{N_y N_z} \sum_{ij} \sum_{\mathbf{k}} \Bigg[& A_{ij} e^{i\mathbf{k}\cdot(\mathbf{r}_j - \mathbf{r}_i)} a^\dagger_{\mathbf{k}}(x_i) a^\dagger_{\mathbf{k}}(x_j) \\
& + \frac{B_{ij}}{2} e^{i\mathbf{k}\cdot(\mathbf{r}_i - \mathbf{r}_j)} a_{\mathbf{k}}(x_i) a_{-\mathbf{k}}(x_j) + \frac{B^*_{ij}}{2} e^{i\mathbf{k}\cdot(\mathbf{r}_j - \mathbf{r}_i)} a^\dagger_{\mathbf{k}}(x_i) a^\dagger_{-\mathbf{k}}(x_j) \Bigg] \\
= \sum_{x_i,x_j} \sum_{\mathbf{k}} & \left[A_{\mathbf{k}}(x_{ij}) a^\dagger_{\mathbf{k}}(x_i) a_{\mathbf{k}}(x_j) + \frac{B_{\mathbf{k}}(x_{ij})}{2} a_{\mathbf{k}}(x_i) a_{-\mathbf{k}}(x_j) + \frac{B^*_{\mathbf{k}}(x_{ij})}{2} a^\dagger_{\mathbf{k}}(x_i) a^\dagger_{-\mathbf{k}}(x_j) \right],
\end{aligned}$$

where have used the orthogonality relation in the third and fourth line. We conclude that equation (4) indeed holds which is in line with Ref. [6]. Now we consider the dipole terms in the amplitude factors. Per definition of the Fourier transformation we have

$$\begin{aligned} D_{\mathbf{k}}^{\alpha\beta}(x_{ij}) &= {\sum_{\mathbf{r}_{ij}}}' e^{-i\mathbf{k}\cdot\mathbf{r}_{ij}} D_{ij}^{\alpha\beta} \\ &= -\mu^2 {\sum_{y_{ij},z_{ij}}}' e^{-i(k_y y_{ij}+k_z z_{ij})} \left[\frac{\delta^{\alpha\beta}}{\left(x_{ij}^2+y_{ij}^2+z_{ij}^2\right)^{3/2}} - \frac{3r_{ij}^{\alpha} r_{ij}^{\beta}}{\left(x_{ij}^2+y_{ij}^2+z_{ij}^2\right)^{5/2}} \right]. \end{aligned} \tag{5}$$

It is necessary to use the Ewald summation for these dipole sums to simulate the situation numerically. We will also verify this in the next chapter which is about the numerical approach of the experiment. To make use of the Ewald summation let us first define

$$I_{\mathbf{k}} = \mu^2 \sum_{y_{ij}z_{ij}} \frac{e^{-i(k_y y_{ij}+k_z z_{ij})}}{\left(x_{ij}^2+y_{ij}^2+z_{ij}^2\right)^{5/2}}.$$

Then we have that

$$\begin{aligned} D_{\mathbf{k}}^{xx} &= \left[\frac{\partial^2}{\partial k_y^2} + \frac{\partial^2}{\partial k_z^2} + 2(x_{ij})^2 \right] I_{\mathbf{k}}(x_{ij}); \\ D_{\mathbf{k}}^{yy} &= \left[\frac{\partial^2}{\partial k_z^2} - 2\frac{\partial^2}{\partial k_y^2} - (x_{ij})^2 \right] I_{\mathbf{k}}(x_{ij}); \\ D_{\mathbf{k}}^{zz} &= \left[\frac{\partial^2}{\partial k_y^2} - 2\frac{\partial^2}{\partial k_z^2} - (x_{ij})^2 \right] I_{\mathbf{k}}(x_{ij}); \\ D_{\mathbf{k}}^{xy} &= 3ix_{ij}\frac{\partial}{\partial k_y} I_{\mathbf{k}}(x_{ij}). \end{aligned} \tag{6}$$

Now we will use the identity

$$\frac{4}{3}\sqrt{\frac{\epsilon^5}{\pi}} \int_0^{\infty} \mathrm{d}t\ t^{3/2} e^{-\epsilon\alpha t} = \alpha^{5/2},$$

where $\alpha = x_{ij}^2 + y_{ij}^2 + z_{ij}^2$ and ϵ a variable, to get

$$I_{\mathbf{k}}(x_{ij}) = \sum_{y_{ij},z_{ij}} \frac{4\mu^2}{3}\sqrt{\frac{\epsilon^5}{\pi}} \int_0^{\infty} \mathrm{d}t\ t^{3/2} e^{-x_{ij}^2\epsilon t} e^{-\left(y_{ij}^2+z_{ij}^2\right)\epsilon t} e^{-i(k_y y_{ij}+k_z z_{ij})}.$$

On the interval $[0,1]$ in t we will use

$$\sum_{\mathbf{r}} e^{-\epsilon t|\mathbf{r}|^2} e^{-i\mathbf{k}\cdot\mathbf{r}} = \frac{\pi}{a^2\epsilon t} \sum_{\mathbf{g}} e^{-\frac{|\mathbf{k}+\mathbf{g}|}{4\epsilon t}},$$

which is the Ewald summation. Here $\mathbf{g}$ represents the reciprocal lattice vectors and a is the lattice constant. The a^2 represents the area of the primitive cell of our lattice. We then get

$$\begin{aligned} I_{\mathbf{k}}(x_{ij}) = &\frac{4\mu^2}{3}\frac{\sqrt{\epsilon^3\pi}}{a^2} \int_0^1 dt \sum_{\mathbf{g}} t^{1/2} e^{-\frac{|\mathbf{k}+\mathbf{g}|}{4\epsilon t} - x_{ij}^2\epsilon t} \\ &+ \sum_{y_{ij},z_{ij}} \frac{4\mu^2}{3}\sqrt{\frac{\epsilon^5}{\pi}} \int_1^{\infty} dt\ t^{3/2} \cdot e^{-\left(x_{ij}^2+y_{ij}^2+z_{ij}^2\right)\epsilon t} \cdot e^{-i(k_y y_{ij}+k_z z_{ij})}. \end{aligned}$$

From now on we will for simplicity refer to the first sum as the reciprocal sum and to the second sum as the real sum. Let us continue by considering the Misra function

$$\psi_{\nu}(x) = \int_1^{\infty} \mathrm{d}t\ t^{\nu} e^{-xt}.$$

For $\nu = 3/2$ we can write this as

$$\psi_{3/2}(x) = e^{-x}\frac{3+2x}{2x^2} + \frac{3\sqrt{\pi}\mathrm{Erfc}(\sqrt{x})}{4x^{5/2}}, \tag{7}$$

where Erfc(x) is the complementary error function. By using this in the real sum we get

$$I_{\mathbf{k}}(x_{ij}) = \frac{4\mu^2}{3}\left[\frac{\sqrt{\epsilon^3\pi}}{a^2}\int_0^1 dt \sum_{\mathbf{g}} t^{1/2} e^{-\frac{|\mathbf{k}+\mathbf{g}|}{4\epsilon t} - x_{ij}^2\epsilon t} + \sqrt{\frac{\epsilon^5}{\pi}}\sum_{y_{ij},z_{ij}} \psi_{3/2}\left(|\mathbf{r}_{ij}|^2\epsilon\right) e^{-i(k_y y_{ij}+k_z z_{ij})}\right],$$

where $|\mathbf{r}_{ij}|^2 = x_{ij}^2 + y_{ij}^2 + z_{ij}^2$. The integral in the reciprocal sum can be evaluated as

$$\int_0^1 \mathrm{d}t\; t^{1/2} e^{-\frac{|\mathbf{k}+\mathbf{g}|}{4\epsilon t} - x_{ij}^2\epsilon t} = -\frac{e^{-p^2-q^2}}{q^2} + \frac{\sqrt{\pi}}{4q^3}\left[e^{-2pq}(1+2pq)\mathrm{Erfc}(p-q) + e^{2pq}(-1+2pq)\mathrm{Erfc}(p+q)\right],$$

where $q = x_{ij}\sqrt{\epsilon}$ and $p = \frac{|\mathbf{k}+\mathbf{g}|}{2\sqrt{\epsilon}}$. By some calculation using equation (6) we then get

$$D_{\mathbf{k}}^{xx}(x_{ij}) = \frac{\pi\mu^2}{a^2}\sum_{\mathbf{g}}\left[\frac{8\sqrt{\epsilon}}{3\sqrt{\pi}}e^{-p^2-q^2} - |\mathbf{k}+\mathbf{g}| f(p,q)\right] - \frac{4\mu^2}{3}\sqrt{\frac{\epsilon^5}{\pi}}\sum_{y_{ij},z_{ij}}\left(|\mathbf{r}_{ij}|^2 - 3x_{ij}^2\right)\cos(k_y y_{ij})\cos(k_z z_{ij})\psi_{3/2}\left(|\mathbf{r}_{ij}|^2\epsilon\right),$$

which is the final result of the Ewald summation. Here we defined

$$f(p,q) = e^{-2pq}\mathrm{Erfc}(p-q) + e^{2pq}\mathrm{Erfc}(p+q).$$

Similarly we get

$$D_{\mathbf{k}}^{yy}(x_{ij}) = \frac{\pi\mu^2}{a^2}\sum_{\mathbf{g}}\left[\frac{8\sqrt{\epsilon}}{3\sqrt{\pi}}e^{-p^2-q^2} - \frac{(k_y+g_y)^2}{|\mathbf{k}+\mathbf{g}|}f(p,q)\right] - \frac{4\mu^2}{3}\sqrt{\frac{\epsilon^5}{\pi}}\sum_{y_{ij},z_{ij}}\left(|\mathbf{r}_{ij}|^2 - 3x_{ij}^2\right)\cos(k_y y_{ij})\cos(k_z z_{ij})\psi_{3/2}\left(|\mathbf{r}_{ij}|^2\epsilon\right);$$

$$D_{\mathbf{k}}^{zz}(x_{ij}) = \frac{\pi\mu^2}{a^2}\sum_{\mathbf{g}}\left[\frac{8\sqrt{\epsilon}}{3\sqrt{\pi}}e^{-p^2-q^2} - \frac{(k_z+g_z)^2}{|\mathbf{k}+\mathbf{g}|}f(p,q)\right] - \frac{4\mu^2}{3}\sqrt{\frac{\epsilon^5}{\pi}}\sum_{y_{ij},z_{ij}}\left(|\mathbf{r}_{ij}|^2 - 3x_{ij}^2\right)\cos(k_y y_{ij})\cos(k_z z_{ij})\psi_{3/2}\left(|\mathbf{r}_{ij}|^2\epsilon\right);$$

$$D_{\mathbf{k}}^{xy}(x_{ij}) = i\frac{\pi\mu^2}{a^2}\mathrm{sig}(x_{ij})\sum_{\mathbf{g}}(k_y+g_y)f(p,q) + 4i\mu^2\sqrt{\frac{\epsilon^5}{\pi}}x_{ij}\sum_{y_{ij},z_{ij}} y_{ij}\sin(k_y y_{ij})\cos(k_z z_{ij})\psi_{3/2}\left(|\mathbf{r}_{ij}|^2\epsilon\right).$$

2.2 Hamiltonian of the new lattice

Now we will find the Hamiltonian for a different situaton. We take the amout of layers in the x-direction to be equal to 1. Moreover, we take out strips of infinite length in the y-direction and length La in the z-direction every three sites in the z-direction. The situation is also given in Figure 3.

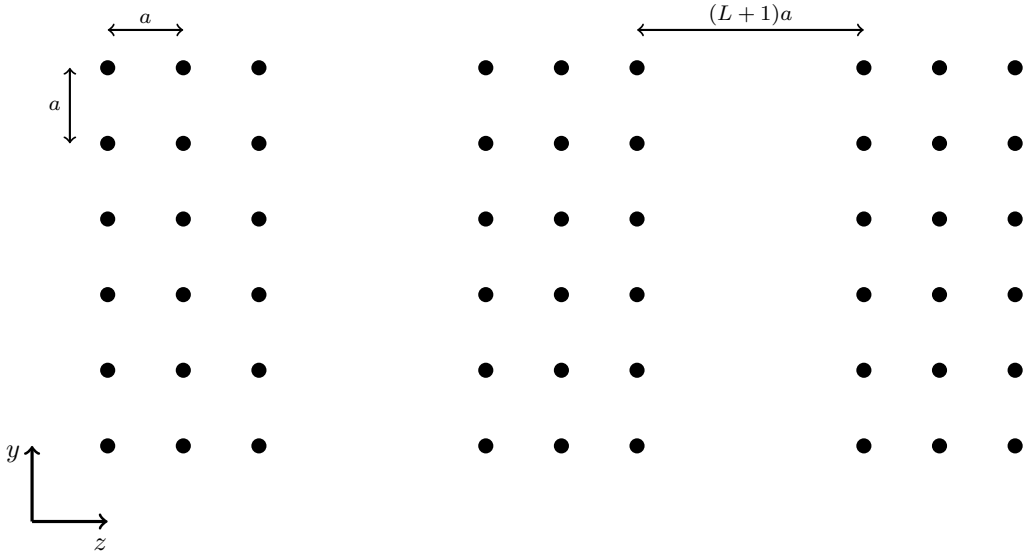

Figure 3: *Simple visualisation of the lattice in the new situation. Every three sites there are L sites removed in the z-direction. The distance between two sites without a hole in between is still* $a = 12.376$ *Å. This drawing is not to scale.*

We still only consider the following quadratic part of the Hamiltonian

$$\hat{H}_2 = \sum_{ij} \left[A_{ij} a_i^\dagger a_j + \frac{B_{ij}}{2} a_i a_j + \frac{B_{ij}^*}{2} a_i^\dagger a_j^\dagger \right]. \tag{8}$$

The difference lies in the fact that we do not have the same translational symmetry in the yz-plane as earlier. Let us define the primive cell as in Figure 4.

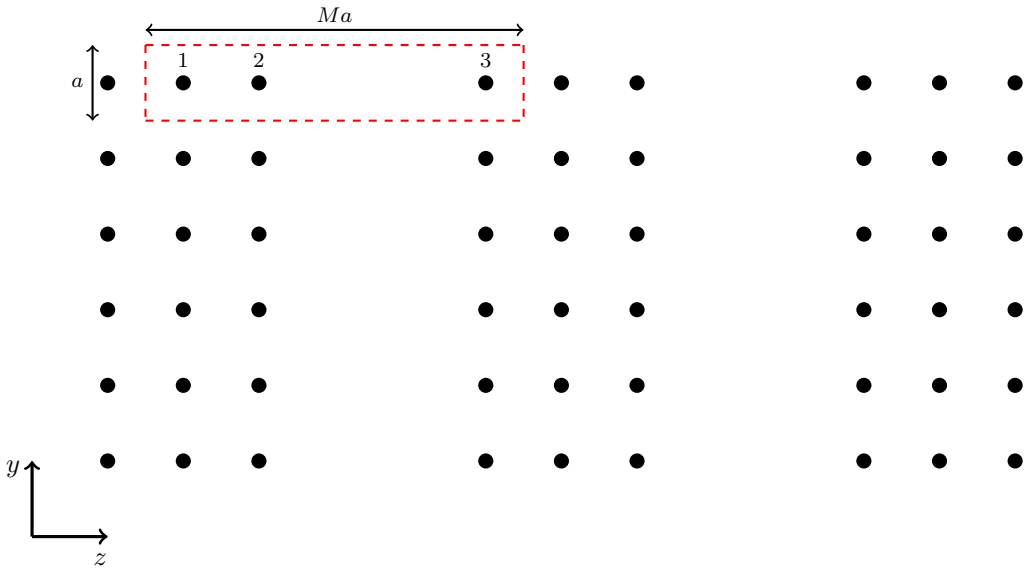

Figure 4: *Simple visualisation of the lattice in the new situation. The primitive cell is indicated by the red dashed line. Each cell is Ma long in the z-direction and a long in the y-direction. Each site in a cell is indicated by a number. Again this drawing is not to scale.*

On the level of cells, however, the lattice does have translational symmetry. Therefore we can apply a Fourier transformation on these cells. As in Figure 4, we have indicated each site in the cell with either 1, 2 or 3. Then we can rewrite the Hamiltonian in the following way,

$$\hat{H}_2 = \sum_{ij}\sum_{nn'}\left[A_{ij}^{nn'}(a_i^n)^\dagger a_j^{n'} + \frac{B_{ij}^{nn'}}{2}a_i^n a_j^{n'} + \frac{B_{ij}^{nn'*}}{2}(a_i^n)^\dagger (a_j^{n'})^\dagger\right],$$

where $\sum_{ij}$ now sums over the cells and $\sum_{nn'}$ sums over the sites within the cell. Using the Fourier transformed annihilation and creation operators we can perform the Fourier transformation in the following way,

$$\begin{aligned}
\hat{H}_2 &= \frac{1}{N^2}\sum_{ij}\sum_{nn'}\sum_{\mathbf{k}\mathbf{k}'}\left[A_{ij}^{nn'}(a_{\mathbf{k}}^n)^\dagger a_{\mathbf{k}'}^{n'} + \frac{B_{ij}^{nn'}}{2}a_{-\mathbf{k}}^n a_{\mathbf{k}'}^{n'} + \frac{B_{ij}^{nn'*}}{2}(a_{\mathbf{k}}^n)^\dagger (a_{-\mathbf{k}'}^{n'})^\dagger\right] e^{-i\mathbf{k}\mathbf{r}_i^n} e^{i\mathbf{k}'\mathbf{r}_j^{n'}} \\
&= \frac{1}{N}\sum_{ij}\sum_{nn'}\sum_{\mathbf{k}}\left[A_{ij}^{nn'}(a_{\mathbf{k}}^n)^\dagger a_{\mathbf{k}}^{n'} + \frac{B_{ij}^{nn'}}{2}a_{-\mathbf{k}}^n a_{\mathbf{k}}^{n'} + \frac{B_{ij}^{nn'*}}{2}(a_{\mathbf{k}}^n)^\dagger (a_{-\mathbf{k}}^{n'})^\dagger\right] e^{i\mathbf{k}\left(\mathbf{r}_j^{n'} - \mathbf{r}_i^n\right)} \\
&= \sum_{nn'}\sum_{\mathbf{k}}\left[A_{\mathbf{k}}^{nn'}(a_{\mathbf{k}}^n)^\dagger a_{\mathbf{k}}^{n'} + \frac{B_{\mathbf{k}}^{nn'}}{2}a_{-\mathbf{k}}^n a_{\mathbf{k}}^{n'} + \frac{B_{\mathbf{k}}^{nn'*}}{2}(a_{\mathbf{k}}^n)^\dagger (a_{-\mathbf{k}}^{n'})^\dagger\right],
\end{aligned}$$

where we have used the orthogonality relation of the discrete Fourier transform in the second line. As we can see this is similar to equation (4), where we sum over the layers instead of the different kind of particles in our cell. The similarity could be explained with the fact that we do not perform a Fourier transformation within the cell and that in (4) we do not perform a Fourier transformation over the layers in the x-direction. For the amplitude factors we get

$$\begin{aligned}
A_{\mathbf{k}}^{nn'} &= \sum_{\mathbf{r}} e^{-i\mathbf{k}\cdot\mathbf{r}} A_{\mathbf{r}0}^{nn'} \\
&= \sum_{\mathbf{r}} e^{-i\mathbf{k}\cdot\mathbf{r}}\left[h\delta_{\mathbf{r}0}^{nn'} + S\left(\delta_{\mathbf{r}0}^{nn'}\sum_{m,\alpha} J_{\mathbf{r},m}^{n\alpha} - J_{\mathbf{r}0}^{nn'}\right)\right. \\
&\quad \left. + S\left(\delta_{\mathbf{r}0}^{nn'}\sum_{m,\alpha} D_{\mathbf{r}m}^{zz,n\alpha} - \frac{D_{\mathbf{r}0}^{xx,nn'} + D_{\mathbf{r}0}^{yy,nn'}}{2}\right)\right].
\end{aligned}$$

where $\sum_{\mathbf{r}}$ sums over the cells. Explicitly for $A_{\mathbf{k}}^{11}$ we see that

$$\begin{aligned}
A_{\mathbf{k}}^{11} &= \sum_{\mathbf{r}} e^{-i\mathbf{k}\cdot\mathbf{r}}\left[h\delta_{\mathbf{r}0} + S\left(\delta_{\mathbf{r}0}\sum_{m,\alpha} J_{\mathbf{r},m}^{1\alpha} - J_{\mathbf{r}0}^{11}\right)\right. \\
&\quad \left. + S\left(\delta_{\mathbf{r}0}\sum_{m,\alpha} D_{\mathbf{r}m}^{zz,1\alpha} - \frac{D_{\mathbf{r}0}^{xx,11} + D_{\mathbf{r}0}^{yy,11}}{2}\right)\right] \\
&= h + S\sum_{m,\alpha} J_{0m}^{1\alpha} - S\sum_{\mathbf{r}} e^{-i\mathbf{k}\cdot\mathbf{r}} J_{\mathbf{r}0}^{11} \\
&\quad + S\sum_{m,\alpha} D_{0m}^{zz,1\alpha} - S\sum_{\mathbf{r}} e^{-i\mathbf{k}\cdot\mathbf{r}}\left(\frac{D_{\mathbf{r}0}^{xx,11} + D_{\mathbf{r}0}^{xx,11}}{2}\right) \\
&= h + 4SJ - SJ_{\mathbf{k}}^{11} + S\sum_{\alpha} D_0^{zz,1\alpha} - \frac{S}{2}\left(D_{\mathbf{k}}^{xx,11} + D_{\mathbf{k}}^{yy,11}\right).
\end{aligned}$$

Similarly, we have

$$
\begin{aligned}
A^{12}_{\mathbf{k}} &= -JS - \frac{S}{2}\left(D^{xx,12}_{\mathbf{k}} + D^{yy,12}_{\mathbf{k}}\right);\\
A^{13}_{\mathbf{k}} &= -e^{-ik_y a} - \frac{S}{2}\left(D^{xx,13}_{\mathbf{k}} + D^{yy,13}_{\mathbf{k}}\right);\\
A^{21}_{\mathbf{k}} &= -JS - \frac{S}{2}\left(D^{xx,21}_{\mathbf{k}} + D^{yy,21}_{\mathbf{k}}\right);\\
A^{22}_{\mathbf{k}} &= h + 3SJ - SJ^{22}_{\mathbf{k}} + S\sum_{\alpha} D^{zz,2\alpha}_{0} - \frac{S}{2}\left(D^{xx,22}_{\mathbf{k}} + D^{yy,22}_{\mathbf{k}}\right);\\
A^{23}_{\mathbf{k}} &= -\frac{S}{2}\left(D^{xx,13}_{\mathbf{k}} + D^{yy,13}_{\mathbf{k}}\right);\\
A^{31}_{\mathbf{k}} &= -e^{ik_y a} - \frac{S}{2}\left(D^{xx,31}_{\mathbf{k}} + D^{yy,31}_{\mathbf{k}}\right);\\
A^{32}_{\mathbf{k}} &= -\frac{S}{2}\left(D^{xx,13}_{\mathbf{k}} + D^{yy,13}_{\mathbf{k}}\right);\\
A^{33}_{\mathbf{k}} &= h + 3SJ - SJ^{22}_{\mathbf{k}} + S\sum_{\alpha} D^{zz,2\alpha}_{0} - \frac{S}{2}\left(D^{xx,22}_{\mathbf{k}} + D^{yy,22}_{\mathbf{k}}\right),
\end{aligned}
$$

and,

$$
B^{nn'}_{\mathbf{k}} = -\frac{S}{2}\left[D^{xx,nn'}_{\mathbf{k}} - 2iD^{xy,nn'}_{\mathbf{k}} - D^{xx,nn'}_{\mathbf{k}}\right].
$$

What remains to be evaluated are the exchange terms $J^{nn'}_{\mathbf{k}}$ and dipole terms $D^{\alpha\beta,nn'}_{\mathbf{k}}$ in $A^{nn'}_{\mathbf{k}}$ and $B^{nn'}_{\mathbf{k}}$. It holds that $J^{nn'}_{k}$ is the Fourier transform of $J^{nn'}_{ij}$, so we have that

$$
\begin{aligned}
J^{nn'}_{\mathbf{k}} &= \frac{1}{N}\sum_{ij} J^{nn'}_{ij} e^{-i\mathbf{k}\cdot\left(\mathbf{r}^{n}_{i} - \mathbf{r}^{n'}_{j}\right)}\\
&= \sum_{i} J^{nn'}_{i0} e^{-i\mathbf{k}\cdot\left(r^{n}_{i} - r^{n'}_{0}\right)},
\end{aligned}
$$

where i indicates the cells and 0 indicate the origin cell. For example we have

$$
J^{11}_{\mathbf{k}} = \sum_{i} J^{11}_{i0} e^{-i\mathbf{k}\cdot\left(\mathbf{r}^{1}_{i} - \mathbf{r}^{1}_{0}\right)}.
$$

Note that a pair of particles of type 1 are only nearest neighbors if they are situated in neighbouring cells in the y-direction. Then $\mathbf{k}\cdot\left(\mathbf{r}^{1}_{i} - \mathbf{r}^{1}_{0}\right)$ will be equal to $\pm k_y a$, which results in the following

$$
\begin{aligned}
J^{11}_{\mathbf{k}} &= J\left(e^{ik_y a} + e^{-ik_y a}\right)\\
&= 2J\cos(k_y a).
\end{aligned}
$$

In a similar way we get the following matrix

$$
\bar{J}_{\mathbf{k}} = \begin{pmatrix} J^{11}_{\mathbf{k}} & J^{12}_{\mathbf{k}} & J^{13}_{\mathbf{k}} \\ J^{21}_{\mathbf{k}} & J^{22}_{\mathbf{k}} & J^{23}_{\mathbf{k}} \\ J^{31}_{\mathbf{k}} & J^{32}_{\mathbf{k}} & J^{33}_{\mathbf{k}} \end{pmatrix} = \begin{pmatrix} 2J\cos(k_y a) & J & Je^{-ik_z Ma} \\ J & 2J\cos(k_y a) & 0 \\ Je^{ik_z Ma} & 0 & 2J\cos(k_y a) \end{pmatrix}.
$$

And now the dipole terms. Let us first consider $D^{xx,nn'}_{\mathbf{k}}$:

$$
D^{xx,nn'}_{\mathbf{k}} = {\sum_{\mathbf{r}_{ij}}}' e^{-i\mathbf{k}\cdot\mathbf{r}_{ij}} D^{xx,nn'}_{ij} \tag{9}
$$

$$
= -\mu^2 {\sum_{y_{ij},z_{ij}}}' e^{-i(k_y y_{ij} + k_z z_{ij})} \left[\frac{1}{\left(\left(x^{nn'}_{ij}\right)^2 + \left(y^{nn'}_{ij}\right)^2 + \left(z^{nn'}_{ij}\right)^2\right)^{3/2}} - \frac{3x^{nn'}_{ij}x^{nn'}_{ij}}{\left(\left(x^{nn'}_{ij}\right)^2 + \left(y^{nn'}_{ij}\right)^2 + \left(z^{nn'}_{ij}\right)^2\right)^{5/2}}\right]. \tag{10}
$$

The $x^{nn'}_{ij}$ is not necessary, but we leave it as it is, because then we can follow our reasoning of the previous case more easily. Let us define

$$
I^{nn'}_{\mathbf{k}} := \mu^2 \sum_{y_{ij}z_{ij}} \frac{e^{-i(k_y y_{ij} + k_z z_{ij})}}{\left(\left(x^{nn'}_{ij}\right)^2 + \left(y^{nn'}_{ij}\right)^2 + \left(z^{nn'}_{ij}\right)^2\right)^{5/2}}
$$

such that

$$D_{\mathbf{k}}^{xx,nn'} = \left[\frac{\partial^2}{\partial k_y^2} + \frac{\partial^2}{\partial k_z^2} + 2\left(x_{ij}^{nn'}\right)^2\right] I_{\mathbf{k}}^{nn'}.$$

Similarly we get that

$$D_{\mathbf{k}}^{yy,nn'} = \left[\frac{\partial^2}{\partial k_z^2} - 2\frac{\partial^2}{\partial k_y^2} - \left(x_{ij}^{nn'}\right)^2\right] I_{\mathbf{k}}^{nn'};$$
$$D_{\mathbf{k}}^{zz,nn'} = \left[\frac{\partial^2}{\partial k_y^2} - 2\frac{\partial^2}{\partial k_z^2} - \left(x_{ij}^{nn'}\right)^2\right] I_{\mathbf{k}}^{nn'}.$$

For $nn' = 11$ it holds that $x_{ij}^{11} = x_{ij}$, $y_{ij}^{11} = y_{ij}$ and $z_{ij}^{11} = z_{ij}$, because the distance between two particles of type 1 is the same as the distance between the cells where they are situated in. This implies that

$$\begin{aligned} D_{\mathbf{k}}^{xx,11} &= {\sum_{\mathbf{r}_{ij}}}' e^{-i\mathbf{k}\cdot\mathbf{r}_{ij}} D_{ij}^{xx,11} \\ &= -\mu^2 {\sum_{y_{ij},z_{ij}}}' e^{-i(k_y y_{ij} + k_z z_{ij})} \left[\frac{1}{\left(x_{ij}^2 + y_{ij}^2 + z_{ij}^2\right)^{3/2}} - \frac{3x_{ij}x_{ij}}{\left(x_{ij}^2 + y_{ij}^2 + z_{ij}^2\right)^{5/2}}\right], \end{aligned}$$

which is the same as equation (5) but for a lattice with a $a_y = a$ and $a_z = Ma$. We then may conclude that

$$\begin{aligned} D_{\mathbf{k}}^{xx,11} = \frac{\pi\mu^2}{Ma^2} \sum_{\mathbf{g}} &\left[\frac{8\sqrt{\epsilon}}{3\sqrt{\pi}} e^{-p^2-q^2} - |\mathbf{k}+\mathbf{g}| f(p,q)\right] \\ &- \frac{4\mu^2}{3}\sqrt{\frac{\epsilon^5}{\pi}} \sum_{y_{ij},z_{ij}} \left(|\mathbf{r}_{ij}|^2 - 3x_{ij}^2\right) \cos(k_y y_{ij}) \cos(k_z z_{ij}) \psi_{3/2}\left(|\mathbf{r}_{ij}|^2 \epsilon\right). \end{aligned}$$

With the same reasoning we can see that

$$D_{\mathbf{k}}^{xx,11} = D_{\mathbf{k}}^{xx,22} = D_{\mathbf{k}}^{xx,33}.$$

Now we consider

$$\begin{aligned} D_{\mathbf{k}}^{xx,12} &= {\sum_{\mathbf{r}_{ij}}}' e^{-i\mathbf{k}\cdot\mathbf{r}_{ij}} D_{ij}^{xx,12} \\ &= -\mu^2 {\sum_{y_{ij},z_{ij}}}' e^{-i(k_y y_{ij} + k_z z_{ij})} \left[\frac{1}{\left(\left(x_{ij}^{12}\right)^2 + \left(y_{ij}^{12}\right)^2 + \left(z_{ij}^{12}\right)^2\right)^{3/2}} - \frac{3x_{ij}^{12}x_{ij}^{12}}{\left(\left(x_{ij}^{12}\right)^2 + \left(y_{ij}^{12}\right)^2 + \left(z_{ij}^{12}\right)^2\right)^{5/2}}\right]. \end{aligned}$$

Note that $x_{ij}^{12} = x_{ij}$ and $y_{ij}^{12} = y_{ij}$, but $z_{ij}^{12} = z_{ij} + a$. Due to this we need to change the procedure regarding the Ewald summation a little. We already found that

$$D_{\mathbf{k}}^{xx,12} = \left[\frac{\partial^2}{\partial k_y^2} + \frac{\partial^2}{\partial k_z^2} + 2\left(x_{ij}^{12}\right)^2\right] I_{\mathbf{k}}^{12},$$

where

$$I_{\mathbf{k}}^{12} = \mu^2 \sum_{y_{ij},z_{ij}} \frac{e^{-i(k_y y_{ij} + k_z z_{ij})}}{\left(\left(x_{ij}^{12}\right)^2 + \left(y_{ij}^{12}\right)^2 + \left(z_{ij}^{12}\right)^2\right)^{5/2}}.$$

We then get that

$$I_{\mathbf{k}}^{12} = \mu^2 \sum_{y_{ij},z_{ij}} \frac{e^{-i(k_y y_{ij} + k_z z_{ij})}}{\left(x_{ij}^2 + y_{ij}^2 + (z_{ij}+a)^2\right)^{5/2}}.$$

Similarly as in the normal case we can write $I_{\mathbf{k}}^{12}$ as follows

$$I_{\mathbf{k}}^{12} = \sum_{y_{ij},z_{ij}} \frac{4\mu^2}{3}\sqrt{\frac{\epsilon^5}{\pi}} \int_0^\infty \mathrm{d}t\; t^{3/2} e^{-x_{ij}^2\epsilon t} e^{-\left(y_{ij}^2 + (z_{ij}+a)^2\right)\epsilon t} e^{-i(k_y y_{ij} + k_z z_{ij})}.$$

Next we apply the Ewald summation

$$\sum_{\mathbf{r}} e^{-\epsilon t|\mathbf{r}+\mathbf{a}|^2} e^{-i\mathbf{k}\cdot\mathbf{r}} = \frac{\pi}{Ma^2\epsilon t} \sum_{g} e^{-\frac{|k+g|}{4\epsilon t}} e^{i\mathbf{g}\cdot\mathbf{a}},$$

on the interval $[0,1]$ in t, but this time we take the shift $\mathbf{a} = (0,0,a)^T$ into account. This results in

$$I_{\mathbf{k}}^{12} = \frac{4\mu^2}{3}\left[\frac{\sqrt{\epsilon^3\pi}}{a^2}\int_0^1 dt \sum_{\mathbf{g}} t^{1/2} e^{-\frac{|\mathbf{k}+\mathbf{g}|}{4\epsilon t} - x_{ij}^2\epsilon t} e^{i\mathbf{g}\cdot\mathbf{a}} + \sqrt{\frac{\epsilon^5}{\pi}} \sum_{y_{ij},z_{ij}} \psi_{3/2}\left(|\mathbf{r}_{ij}+\mathbf{a}|^2\epsilon\right) e^{-i(k_y y_{ij}+k_z z_{ij})}\right].$$

By calculating the derivatives we then get that

$$D_{\mathbf{k}}^{xx,12} = \frac{\pi\mu^2}{Ma^2}\sum_{\mathbf{g}} e^{i\mathbf{g}\cdot\mathbf{a}}\left[\frac{8\sqrt{\epsilon}}{3\sqrt{\pi}} e^{-p^2-q^2} - |\mathbf{k}+\mathbf{g}| f(p,q)\right] - \frac{4\mu^2}{3}\sqrt{\frac{\epsilon^5}{\pi}} \sum_{y_{ij},z_{ij}} \left(|\mathbf{r}_{ij}|^2 - 3x_{ij}^2\right)\cos(k_y y_{ij})\cos(k_z z_{ij})\psi_{3/2}\left(|\mathbf{r}_{ij}+\mathbf{a}|^2\epsilon\right). \tag{11}$$

For the other $D_{\mathbf{k}}^{xx,nn'}$ we just get a different shift which are given in Table 1. For $D_{\mathbf{k}}^{yy,nn'}$ and $D_{\mathbf{k}}^{zz,nn'}$ we get

$$D_{\mathbf{k}}^{yy,nn'} = \frac{\pi\mu^2}{Ma^2}\sum_{\mathbf{g}} e^{i\mathbf{g}\cdot\mathbf{a}}\left[\frac{4\sqrt{\epsilon}}{3\sqrt{\pi}} e^{-p^2-q^2} - \frac{(k_y+g_y)^2}{|\mathbf{k}+\mathbf{g}|} f(p,q)\right] - \frac{4\mu^2}{3}\sqrt{\frac{\epsilon^5}{\pi}} \sum_{y_{ij},z_{ij}} \left(|\mathbf{r}_{ij}|^2 - 3y_{ij}^2\right)\cos(k_y y_{ij})\cos(k_z z_{ij})\psi_{3/2}\left(|\mathbf{r}_{ij}+\mathbf{a}|^2\epsilon\right);$$

$$D_{\mathbf{k}}^{zz,nn'} = \frac{\pi\mu^2}{Ma^2}\sum_{\mathbf{g}} e^{i\mathbf{g}\cdot\mathbf{a}}\left[\frac{4\sqrt{\epsilon}}{3\sqrt{\pi}} e^{-p^2-q^2} - \frac{(k_z+g_z)^2}{|\mathbf{k}+\mathbf{g}|} f(p,q)\right] - \frac{4\mu^2}{3}\sqrt{\frac{\epsilon^5}{\pi}} \sum_{y_{ij},z_{ij}} \left(|\mathbf{r}_{ij}|^2 - 3z_{ij}^2\right)\cos(k_y y_{ij})\cos(k_z z_{ij})\psi_{3/2}\left(|\mathbf{r}_{ij}+\mathbf{a}|^2\epsilon\right),$$

where we take the shift $\mathbf{a}$ also according to Table 1. Now we set $x_{ij}^{nn'}$ to zero, as we consider only one layer in the x-direction. Because of this the $D_{\mathbf{k}}^{xy,nn'}$ will vanish. In the following chapter we will discuss the validity of the Ewald summation and we will discuss on how to numerically diagonalize the Hamiltonians.

Table 1: *The shift* $\mathbf{a}$ *for each* nn' *in* $D_{\boldsymbol{k}}^{\alpha\beta,nn'}$. *Here we have* $a = 12.376$ *Å.*

nn'	$\mathbf{a}$
11	$(0,0,0)^T$
12	$(0,0,a)^T$
13	$(0,0,-a)^T$
21	$(0,0,-a)^T$
22	$(0,0,0)^T$
23	$(0,0,-2a)^T$
31	$(0,0,a)^T$
32	$(0,0,2a)^T$
33	$(0,0,0)^T$

2.3 Diagonalization

In this section we will discuss how we will find the eigenvalues of our Hamiltonian in both cases of the lattice with and without holes. We mainly follow Ref. [9] for this. What we will do, is first writing our Hamiltonian in matrix form, wherafter we perform a basis transformation. Eventually this gives us an eigenvalue problem which we are able to solve, and because of the fact that eigenvalues are invariant under a change of basis we get our dispersion relation. First, we consider the case of the lattice without holes. As we said in Section 2.1 we will only focus on the quadratic part of the Hamiltonian

$$\hat{H}_2 = \sum_{x_i,x_j}\sum_{\mathbf{k}}\left[A_{\mathbf{k}}(x_{ij})a^\dagger_{\mathbf{k}}(x_i)a_{\mathbf{k}}(x_j) + \frac{B_{\mathbf{k}}(x_{ij})}{2}a_{\mathbf{k}}(x_i)a_{-\mathbf{k}}(x_j) + \frac{B^*_{\mathbf{k}}(x_{ij})}{2}a^\dagger_{\mathbf{k}}(x_i)a^\dagger_{-\mathbf{k}}(x_j)\right].$$

We can also write this as

$$\begin{aligned}\hat{H}_2 &= \sum_{\mathbf{k}}\sum_{x_i,x_j}\left[\frac{A_{\mathbf{k}}(x_{ij})}{2}a^\dagger_{\mathbf{k}}(x_i)a_{\mathbf{k}}(x_j) + \frac{A_{\mathbf{k}}(x_{ij})}{2}a_{-\mathbf{k}}(x_i)a^\dagger_{-\mathbf{k}}(x_j)\right.\\ &\quad\left. + \frac{B_{\mathbf{k}}(x_{ij})}{2}a_{\mathbf{k}}(x_i)a_{-\mathbf{k}}(x_j) + \frac{B^*_{\mathbf{k}}(x_{ij})}{2}a^\dagger_{\mathbf{k}}(x_i)a^\dagger_{-\mathbf{k}}(x_j)\right]\\ &= \sum_{\mathbf{k}}\hat{H}_2^{\mathbf{k}},\end{aligned}$$

where we defined

$$\begin{aligned}\hat{H}_2^{\mathbf{k}} &= \sum_{x_i,x_j}\left[\frac{A_{\mathbf{k}}(x_{ij})}{2}a^\dagger_{\mathbf{k}}(x_i)a_{\mathbf{k}}(x_j) + \frac{A_{\mathbf{k}}(x_{ij})}{2}a_{-\mathbf{k}}(x_i)a^\dagger_{-\mathbf{k}}(x_j)\right.\\ &\quad\left. + \frac{B_{\mathbf{k}}(x_{ij})}{2}a_{\mathbf{k}}(x_i)a_{-\mathbf{k}}(x_j) + \frac{B^*_{\mathbf{k}}(x_{ij})}{2}a^\dagger_{\mathbf{k}}(x_i)a^\dagger_{-\mathbf{k}}(x_j)\right].\end{aligned}$$

This will be the expression we want to diagonalize. Calculating the eigenvalues as a function of the wavevector k gives us the dispersion relation. Now let us define

$$\vec{a}_{\mathbf{k}} := \begin{pmatrix} a_{\mathbf{k}}(x_1)\\ a_{\mathbf{k}}(x_2)\\ \vdots\\ a_{\mathbf{k}}(x_N)\end{pmatrix},$$

and,

$$\bar{A}_{\mathbf{k}} := \begin{pmatrix} A_{\mathbf{k}}(x_{11}) & A_{\mathbf{k}}(x_{12}) & \dots & A_{\mathbf{k}}(x_{1N})\\ A_{\mathbf{k}}(x_{21}) & A_{\mathbf{k}}(x_{22}) & \dots & A_{\mathbf{k}}(x_{2N})\\ \vdots & \vdots & \ddots & \vdots\\ A_{\mathbf{k}}(x_{N1}) & A_{\mathbf{k}}(x_{N2}) & \dots & A_{\mathbf{k}}(x_{NN})\end{pmatrix};$$

$$\bar{B}_{\mathbf{k}} := \begin{pmatrix} B_{\mathbf{k}}(x_{11}) & B_{\mathbf{k}}(x_{12}) & \dots & B_{\mathbf{k}}(x_{1N})\\ B_{\mathbf{k}}(x_{21}) & B_{\mathbf{k}}(x_{22}) & \dots & B_{\mathbf{k}}(x_{2N})\\ \vdots & \vdots & \ddots & \vdots\\ B_{\mathbf{k}}(x_{N1}) & B_{\mathbf{k}}(x_{N2}) & \dots & B_{\mathbf{k}}(x_{NN})\end{pmatrix}.$$

Then we write $\hat{H}_2^{\mathbf{k}}$ as follows,

$$\hat{H}_2^{\mathbf{k}} = \begin{pmatrix}\vec{a}^\dagger_{\mathbf{k}} & \vec{a}_{-\mathbf{k}}\end{pmatrix}\begin{pmatrix}\bar{A}_{\mathbf{k}} & \bar{B}_{\mathbf{k}}\\ \bar{B}^\dagger_{\mathbf{k}} & \bar{A}_{\mathbf{k}}\end{pmatrix}\begin{pmatrix}\vec{a}_{\mathbf{k}}\\ \vec{a}^\dagger_{-\mathbf{k}}\end{pmatrix}, \tag{12}$$

where $\bar{B}^\dagger_{\mathbf{k}}$ stands for the transposed complex conjugate of $\bar{B}_{\mathbf{k}}$. For convenience we define

$$D := \begin{pmatrix}\bar{A}_{\mathbf{k}} & \bar{B}_{\mathbf{k}}\\ \bar{B}^\dagger_{\mathbf{k}} & \bar{A}_{\mathbf{k}}\end{pmatrix}.$$

According to Ref. [9] there exists a transformation $\hat{T}$ such that $(\hat{T}^\dagger)^{-1}D\hat{T}^{-1}$ is a diagonal matrix. This transformation has the additional property that

$$\hat{T}^\dagger\hat{\sigma} = \hat{\sigma}\hat{T}^{-1}, \tag{13}$$

where

$$\hat{\sigma} = \text{diag}(\underbrace{1,\ldots,1}_{N},\underbrace{-1,\ldots,-1}_{N}).$$

Equivalently to equation (12) we then have

$$\begin{aligned}\hat{H}_2 &= \begin{pmatrix}\vec{a}_{\mathbf{k}}^{\dagger} & \vec{a}_{-\mathbf{k}}\end{pmatrix}\hat{T}^{\dagger}(\hat{T}^{\dagger})^{-1}D\hat{T}^{-1}\hat{T}\begin{pmatrix}\vec{a}_{\mathbf{k}}\\ \vec{a}_{-\mathbf{k}}^{\dagger}\end{pmatrix};\\ &= \begin{pmatrix}\vec{c}_{\mathbf{k}}^{\dagger} & \vec{c}_{-\mathbf{k}}\end{pmatrix}(\hat{T}^{\dagger})^{-1}D\hat{T}^{-1}\begin{pmatrix}\vec{c}_{\mathbf{k}}\\ \vec{c}_{-\mathbf{k}}^{\dagger}\end{pmatrix},\end{aligned}$$

with

$$\begin{aligned}\begin{pmatrix}\vec{c}_{\mathbf{k}}^{\dagger} & \vec{c}_{-\mathbf{k}}\end{pmatrix} &= \begin{pmatrix}\vec{a}_{\mathbf{k}}^{\dagger} & \vec{a}_{-\mathbf{k}}\end{pmatrix}\hat{T}^{\dagger};\\ \begin{pmatrix}\vec{c}_{\mathbf{k}}\\ \vec{c}_{-\mathbf{k}}^{\dagger}\end{pmatrix} &= \hat{T}\begin{pmatrix}\vec{a}_{\mathbf{k}}\\ \vec{a}_{-\mathbf{k}}^{\dagger}\end{pmatrix}.\end{aligned} \tag{14}$$

These newly defined operators are still bosonic annihalation and creation operators. So in principle this is just a change of basis. For reasons that become apparent later we define $\lambda_1,\ldots,\lambda_{2N}$ and Λ such that

$$\begin{aligned}(\hat{T}^{\dagger})^{-1}D\hat{T}^{-1} &= \text{diag}(\lambda_1,\ldots,\lambda_N,-\lambda_{N+1},\ldots,-\lambda_{2N})\\ &= \hat{\sigma}\Lambda.\end{aligned}$$

It then follows that

$$\begin{aligned}D\hat{T}^{-1} &= \hat{T}^{\dagger}\hat{\sigma}\Lambda\\ &= \hat{\sigma}\hat{T}^{-1}\Lambda.\end{aligned}$$

We define the N-vectors u_p and v_p such that

$$\hat{T}^{-1} = \begin{pmatrix}u_1 & \ldots & u_{2N}\\ v_1 & \ldots & v_{2N}\end{pmatrix}.$$

For all $p \in \{1,..,2N\}$ we then have the following eigenvalue problem,

$$\begin{pmatrix}\bar{A}_{\mathbf{k}} & \bar{B}_{\mathbf{k}}\\ \bar{B}_{\mathbf{k}}^{\dagger} & \bar{A}_{\mathbf{k}}\end{pmatrix}\begin{pmatrix}u_p\\ v_p\end{pmatrix} = \lambda_p\ \hat{\sigma}\begin{pmatrix}u_p\\ v_p\end{pmatrix}.$$

As we said earlier, these eigenvalues are what we were looking for. To find these we must diagonalize the matrix D. In our numerical research we used the Cholesky decomposition to diagonalize D. The results are given in the next chapter. For the case of the lattice with holes we also only consider the quadratic part of the hamiltonian

$$\begin{aligned}\hat{H}_2 &= \sum_{nn'}\sum_{\mathbf{k}}\left[A_{\mathbf{k}}^{nn'}(a_{\mathbf{k}}^{n})^{\dagger}a_{\mathbf{k}}^{n'} + A_{\mathbf{k}}^{nn'}a_{-\mathbf{k}}^{n}a_{-\mathbf{k}}^{n'\dagger} + \frac{B_{\mathbf{k}}^{nn'}}{2}a_{\mathbf{k}}^{n}a_{-\mathbf{k}}^{n'} + \frac{B_{\mathbf{k}}^{nn'*}}{2}(a_{\mathbf{k}}^{n})^{\dagger}(a_{-\mathbf{k}}^{n'})^{\dagger}\right]\\ &= \sum_{\mathbf{k}}\hat{H}_2^{\mathbf{k}}.\end{aligned}$$

We define

$$\begin{aligned}\vec{a}_{\mathbf{k}} &:= \begin{pmatrix}a_{\mathbf{k}}^{1}\\ a_{\mathbf{k}}^{2}\\ a_{\mathbf{k}}^{3}\end{pmatrix};\\ \bar{A}_{\mathbf{k}} &:= \begin{pmatrix}A_{\mathbf{k}}^{11} & A_{\mathbf{k}}^{12} & A_{\mathbf{k}}^{13}\\ A_{\mathbf{k}}^{21} & A_{\mathbf{k}}^{22} & A_{\mathbf{k}}^{23}\\ A_{\mathbf{k}}^{31} & A_{\mathbf{k}}^{32} & A_{\mathbf{k}}^{33}\end{pmatrix};\\ \bar{B}_{\mathbf{k}} &:= \begin{pmatrix}B_{\mathbf{k}}^{11} & B_{\mathbf{k}}^{12} & B_{\mathbf{k}}^{13}\\ B_{\mathbf{k}}^{21} & B_{\mathbf{k}}^{22} & B_{\mathbf{k}}^{23}\\ B_{\mathbf{k}}^{31} & B_{\mathbf{k}}^{32} & B_{\mathbf{k}}^{33}\end{pmatrix},\end{aligned}$$

so that we then get

$$\hat{H}_2 = \begin{pmatrix}\vec{a}_{\mathbf{k}}^{\dagger} & \vec{a}_{-\mathbf{k}}\end{pmatrix}\begin{pmatrix}\bar{A}_{\mathbf{k}} & \bar{B}_{\mathbf{k}}\\ \bar{B}_{\mathbf{k}}^{\dagger} & \bar{A}_{\mathbf{k}}\end{pmatrix}\begin{pmatrix}\vec{a}_{\mathbf{k}}\\ \vec{a}_{-\mathbf{k}}^{\dagger}\end{pmatrix},$$

which is the same as equation (12). We then repeat the same procedure to find the eigenvalues of the system. These results are also given in the next chapter.

3 Numerical method and results

In this chapter we discuss the numerical results of our research. We start by discussing the Ewald summation and afterwards we explain how we diagonalized the Hamiltonians. Finally, we show the dispersion relations. For our simulations we used the programming language Julia.

3.1 Ewald summation

In this section we show that using the Ewald summation makes our simulations more efficient. We will do this for both situations, for the lattice with and without holes.

3.1.1 Comparison in the old case

Let us start where we finished Section 2.1, with the dipole term $D^{xx}_{\mathbf{k}}(x_{ij})$ where we used the Ewald summation which is given by

$$D^{xx}_{\mathbf{k}}(x_{ij}) = \frac{\pi\mu^2}{a^2}\sum_{\mathbf{g}}\left[\frac{8\sqrt{\epsilon}}{3\sqrt{\pi}}e^{-p^2-q^2} - |\mathbf{k}+\mathbf{g}|f(p,q)\right] \\ - \frac{4\mu^2}{3}\sqrt{\frac{\epsilon^5}{\pi}}\sum_{y_{ij},z_{ij}}\left(|\mathbf{r}_{ij}|^2 - 3x_{ij}^2\right)\cos(k_y y_{ij})\cos(k_z z_{ij})\psi_{3/2}\left(|\mathbf{r}_{ij}|^2\epsilon\right).$$

The original dipole term $D^{xx}_{\mathbf{k}}(x_{ij})$ is given by

$$D^{xx}_{\mathbf{k}}(x_{ij}) = -\mu^2 {\sum_{y_{ij},z_{ij}}}' e^{-i(k_y y_{ij}+k_z z_{ij})}\left[\frac{1}{\left(x_{ij}^2+y_{ij}^2+z_{ij}^2\right)^{3/2}} - \frac{3x_{ij}^2}{\left(x_{ij}^2+y_{ij}^2+z_{ij}^2\right)^{5/2}}\right].$$

From now on we call these the Ewald dipole term and the explicit dipole term respectively. We consider the lattice without holes with only one layer. Therefore the only possibility for the variable x_{ij} is $x_{ij} = 0$. Furthermore, we only consider spin waves in the z-direction. For μ we have $\mu = g\mu_B$ and here we take $g = 2$ and μ_B to be the Bohr magneton like in Ref. [6]. We are free to choose the parameter ϵ, so we choose it to be equal to a^{-2}, because this gives us the best results. The reason that this gives the best results is because of the Misra function. As we could see in equation (7) there is an exponential in the Misra function and without considering the ϵ the exponent is in the order of a^2. Computers find it hard to evaluate large or small exponents. That is why we choose $\epsilon = a^{-2}$, such that the exponent is in the order of 1. It is numerically impossible to simulate a lattice of infinite length in the y- and z-direction, so that is why we only consider finite lengths. Note that the expression inside the sum of the explicit dipole terms goes as r^{-3}, where r is the distance of a site to the origin. This means that the sum converges to a certain value as the size of the lattice increases. So we have that both dipole terms of a finite lattice are an approximation of the explicit dipole term of the infinite lattice and the approximation gets better if we consider a larger lattice. For simplicity we will only look at a square lattice, so we define N such that

$$2N + 1 := N_y = N_z. \tag{15}$$

For the terms in the real sums we then have

$$y_{ij} \in \{-N, \ldots, -1, 0, 1, \ldots, N\} \\ z_{ij} \in \{-N, \ldots, -1, 0, 1, \ldots, N\},$$

as we take the origin in the middle of the film. Our initial thought would be that the dipole terms will be more accurate if N increases. To verify this thought we plotted the explicit dipole terms as a function of N in Figure 5(a) and Figure 6(a) for respectively

$$k_y = 0 \text{ cm}^{-1}; \\ k_z = 10^2 \text{ cm}^{-1},$$

and

$$k_y = 0 \text{ cm}^{-1}; \\ k_z = 10^7 \text{ cm}^{-1}.$$

Besides that we put the Ewald dipole terms next to it where we keep $N_{\text{Ewald}} = 10$ constant. We see that for $k_z = 10^2$ cm^{-1} the explicit dipole terms after $N = 2000$ are similar to a value which the Ewald dipole term is already on. More precisely, the difference is in the order of 10^{-5} GHz while the dipole terms are in the order of 10^{-2} GHz. This means that we get about the same result if we choose the explicit dipole term with N larger than 2000 and the Ewald dipole term with $N_{\text{Ewald}} = 10$. In Figure 6 we see that the explicit dipole terms after $N = 600$ are similar to the Ewald dipole term. Here the difference is in the order of 10^{-7} GHz. while the dipole terms are in the order of 10^{-2} GHz. We observe that the explicit dipole terms converge faster for large spin waves, but still, the Ewald dipole term only needs $N_{\text{Ewald}} = 10$. To exploit this advantage we used the Ewald summation for a lattice of 21 by 21 sites in our research. We have plotted $D_{\mathbf{k}}^{yy}$ and $D_{\mathbf{k}}^{zz}$ in the same figures with the same parameters. For these it also holds that the explicit dipole term converges to the value of the Ewald dipole term. We did not plot $D_{\mathbf{k}}^{xy}$ as this term vanishes because $x_{ij} = 0$.

3.1.2 Comparison in the new case

We finished Section 2.2 with

$$D_{\mathbf{k}}^{xx,nn'} = \frac{\pi\mu^2}{Ma^2}\sum_{\mathbf{g}} e^{i\mathbf{g}\cdot\mathbf{a}}\left[\frac{8\sqrt{\epsilon}}{3\sqrt{\pi}}e^{-p^2-q^2} - |\mathbf{k}+\mathbf{g}|f(p,q)\right] - \frac{4\mu^2}{3}\sqrt{\frac{\epsilon^5}{\pi}}\sum_{y_{ij},z_{ij}}\left(|\mathbf{r}_{ij}|^2 - 3x_{ij}^2\right)\cos(k_y y_{ij})\cos(k_z z_{ij})\psi_{3/2}\left(|\mathbf{r}_{ij}+\mathbf{a}|^2\epsilon\right),$$

which is the result of the Ewald summation applied on

$$\begin{aligned} D_{\mathbf{k}}^{xx,nn'} &= {\sum_{\mathbf{r}_{ij}}}' e^{-i\mathbf{k}\cdot\mathbf{r}_{ij}} D_{ij}^{xx,nn'} \\ &= -\mu^2 {\sum_{y_{ij},z_{ij}}}' e^{-i(k_y y_{ij}+k_z z_{ij})}\left[\frac{1}{\left(\left(x_{ij}^{nn'}\right)^2+\left(y_{ij}^{nn'}\right)^2+\left(z_{ij}^{nn'}\right)^2\right)^{3/2}} - \frac{3x_{ij}^{nn'}x_{ij}^{nn'}}{\left(\left(x_{ij}^{nn'}\right)^2+\left(y_{ij}^{nn'}\right)^2+\left(z_{ij}^{nn'}\right)^2\right)^{5/2}}\right]. \end{aligned}$$

Now we take the length of the cell in the z-direction to be $M = 10$ and all other parameters the same as earlier, but this time with a shift

$$\mathbf{a} = (0, 0, a)^T.$$

We can see in Figure 7(a) that for $k_z = 10^2$ cm^{-1} the explicit dipole terms need an N of at least 1500 to be similar to the Ewald dipole term with $N_{\text{Ewald}} = 20$ this time. This is also the case for $D_{\mathbf{k}}^{yy,nn'}$ and $D_{\mathbf{k}}^{zz,nn'}$ in Figures 7(b) and 7(c). For $D_{\mathbf{k}}^{zz,nn'}$ we can see a difference between the graphs of the explicit and Ewald dipole term. However, for $N = 2000$ this is a difference in the order of 10^{-8} GHz while the dipole terms themselves are in the order 10^{-2} GHz. The differences for $D^{xx,nn'}$ and $D^{yy,nn'}$ are in the order of 10^{-6} GHz. In Figure 8 we see that the explicit dipole terms now converge faster to the Ewald dipole term just as in the old case compared to the dipole terms in Figure 7. For N larger than 400 the difference between the dipole terms are in the order of 10^{-10} GHz for $D_{\mathbf{k}}^{xx,nn'}$. To exploit the fact that $N_{\text{Ewald}} = 20$ we use the Ewald dipole term with a lattice of 41 by 41 in our simulations next section.

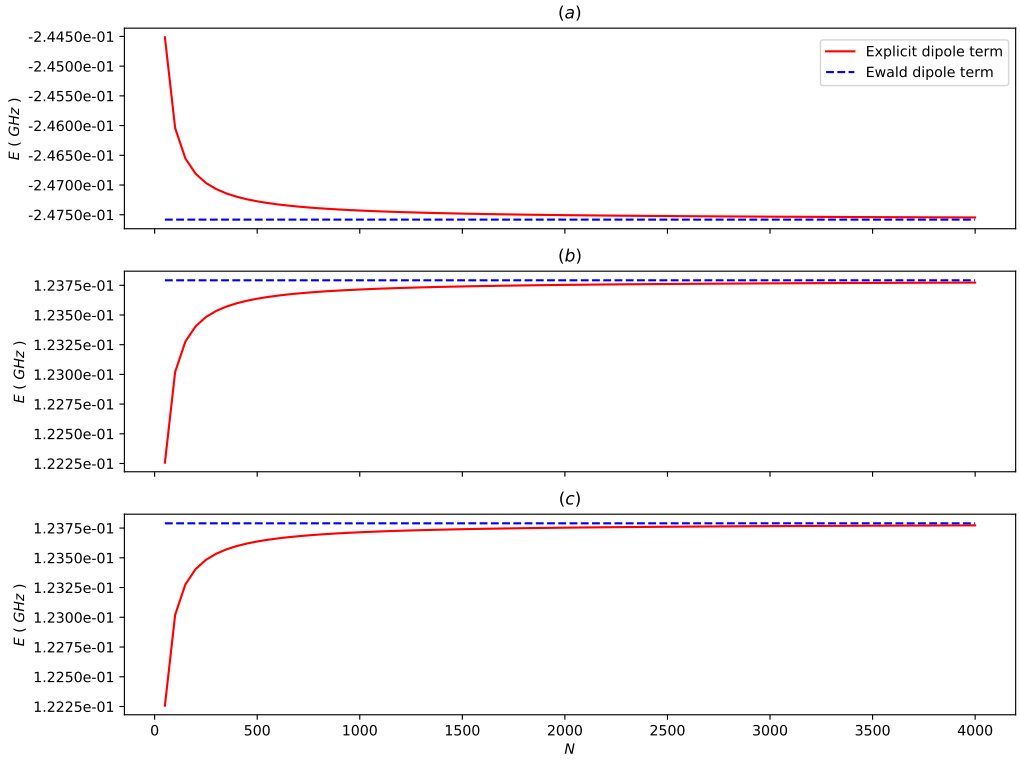

Figure 5: *The relation between the explicit dipole term and N as defined in (15) for $k_z = 10^2$ cm^{-1}. The dashed blue lines are the Ewald dipole terms with $N_{Ewald} = 10$. The upper one is $D_{\boldsymbol{k}}^{xx}$, the middle one is $D_{\boldsymbol{k}}^{yy}$ and the lower one is $D_{\boldsymbol{k}}^{zz}$ indicated by (a), (b) and (c) respectively. In this situation we consider only one layer.*

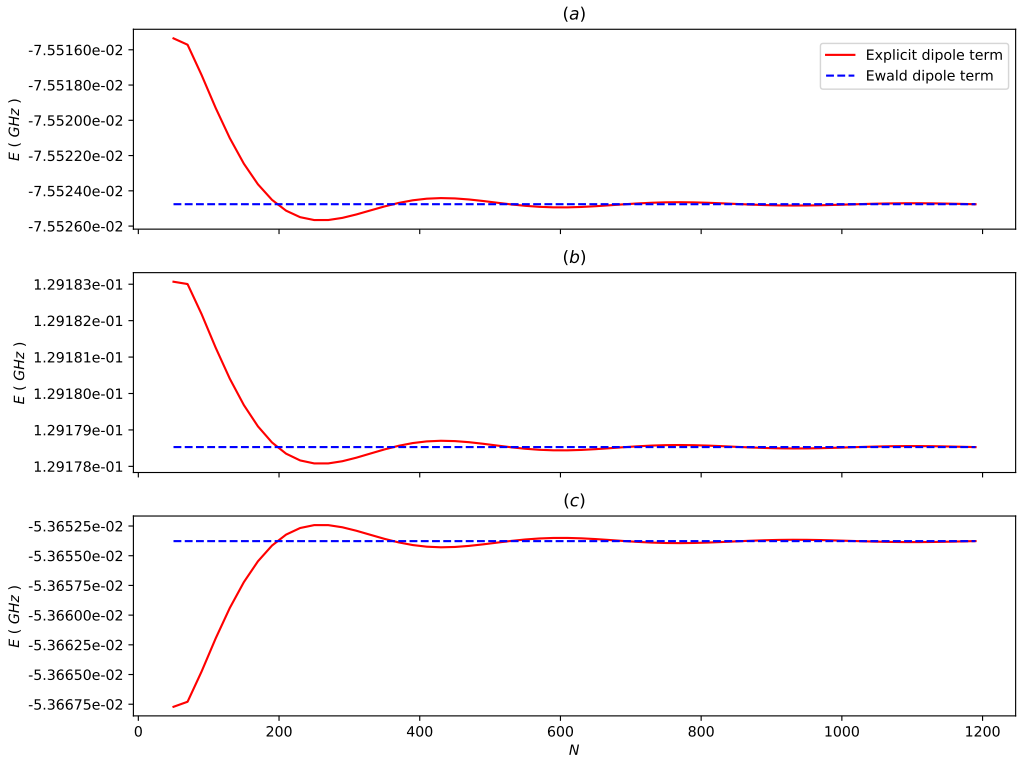

Figure 6: *The relation between the explicit dipole term and N as defined in (15) for $k_z = 10^7$ cm^{-1}. The dashed blue lines are the Ewald dipole terms with $N_{Ewald} = 10$. The upper one is $D_{\boldsymbol{k}}^{xx}$, the middle one is $D_{\boldsymbol{k}}^{yy}$ and the lower one is $D_{\boldsymbol{k}}^{zz}$ indicated by (a), (b) and (c) respectively. In this situation we consider only one layer.*

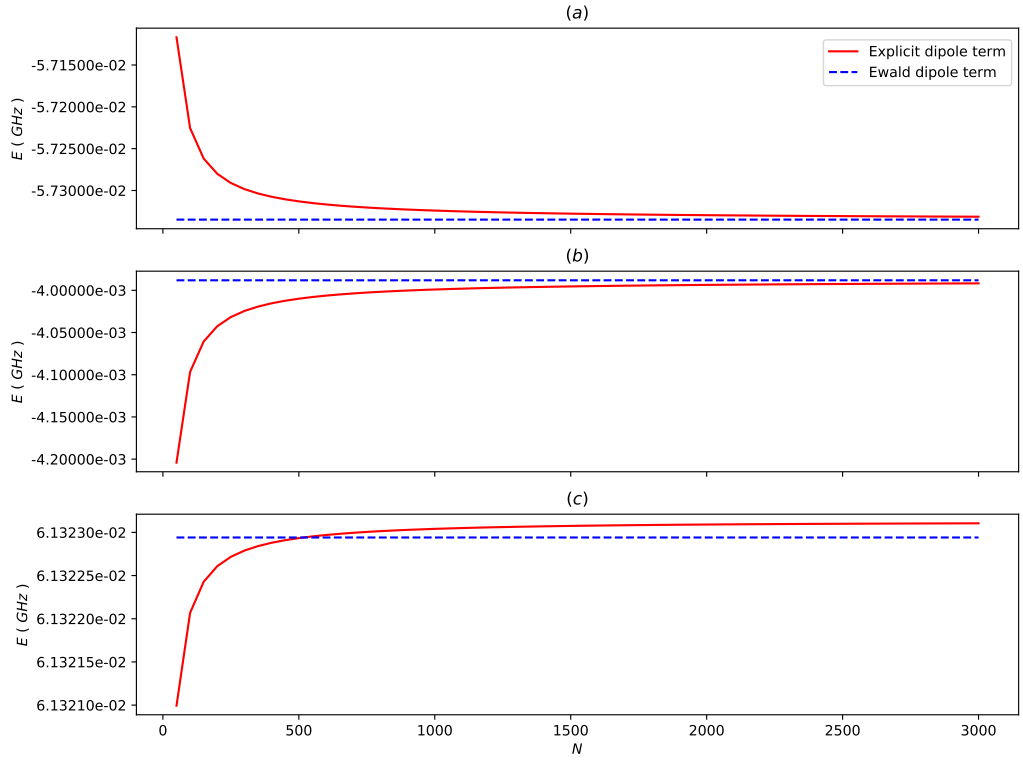

Figure 7: *The relation between the shifted explicit dipole term and N as defined in (15) for $k_z = 10^2$ cm^{-1} represented with the red line. The blue dashed line is the shifted Ewald dipole term with $N_{Ewald} = 20$. The upper one is $D_{\boldsymbol{k}}^{xx,nn'}$, the middle one is $D_{\boldsymbol{k}}^{yy,nn'}$ and the lower one is $D_{\boldsymbol{k}}^{zz,nn'}$ indicated by (a), (b) and (c) respectively. The shift is chosen to be $\boldsymbol{a} = (0, 0, a)^T$. In this situation we consider only one layer.*

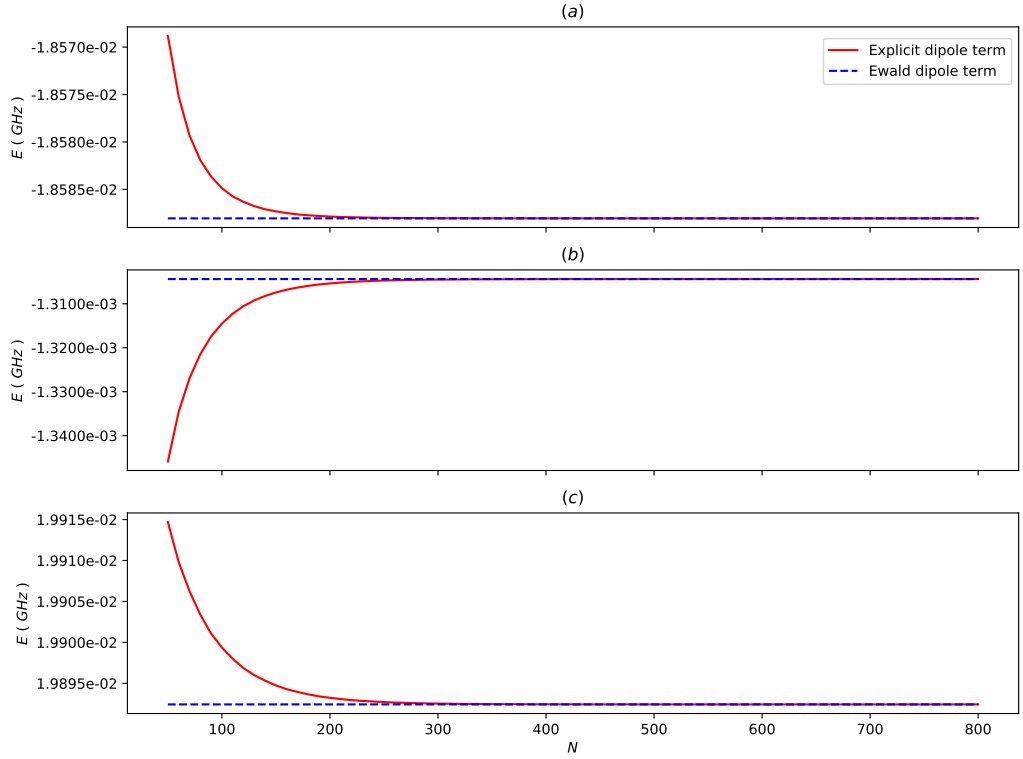

Figure 8: *The relation between the shifted explicit dipole term and N as defined in (15) for $k_z = 10^7$ cm^{-1} represented with the red line. The upper one is $D_{\boldsymbol{k}}^{xx,nn'}$, the middle one is $D_{\boldsymbol{k}}^{yy,nn'}$ and the lower one is $D_{\boldsymbol{k}}^{zz,nn'}$ indicated by (a), (b) and (c) respectively. The shift is chosen to be $\boldsymbol{a} = (0, 0, a)^T$. The dashed blue line is the shifted Ewald dipole term with $N_{Ewald} = 20$. In this situation we consider only one layer.*

3.2 Results

In this section we present the results of our research. This includes the dispersion relation of the lattice with and without holes. In Figure 9 the dispersion relation of a YIG film without holes is given. We used the same parameters and theory as in Ref. [6] and, as expected, we obtained the same result. What we can see is that the relation has a minimum around $k_z = 10^5$ cm^{-1} for the lower eigenstates. Instead of 400 layers we also plotted the same relation for one layer for wavevectors in the first four Brillouin zones which can be seen in Figure 10. In this case we only have one eigenstate, because we have one layer. The behaviour is as expected, because the dispersion relation is periodic with a period of $\frac{2\pi}{a}$. The reason we show this, is because we encountered a similar behaviour in the dispersion relation for a YIG film with holes where we neglect the exchange interaction. This can be seen in Figure 12. The dispersion relation where we do consider the exchange interaction is given in Figure 11.

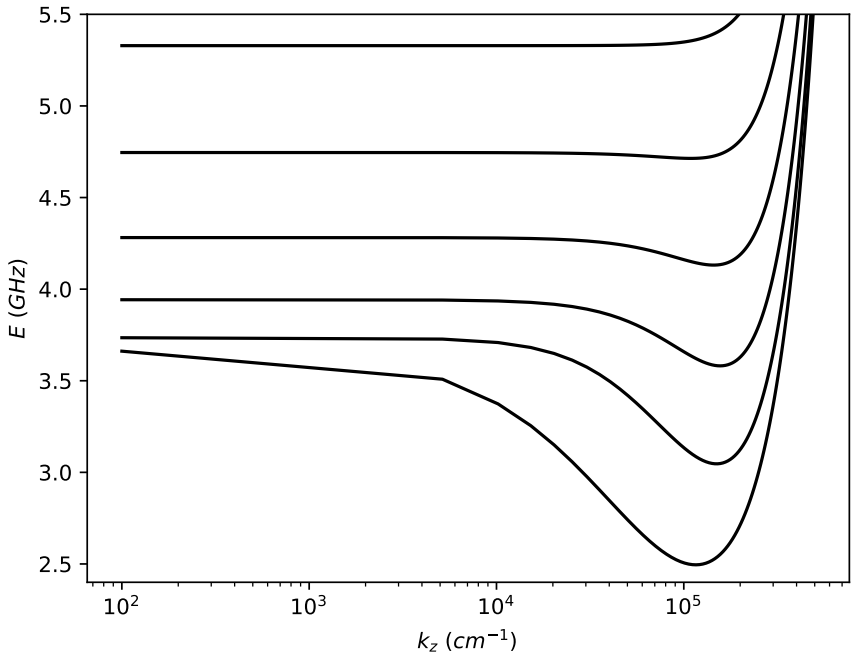

Figure 9: *Dispersion relation for a YIG film without holes plotted on a logarithmic scale. The lattice has 400 layers and the external magnetic field is 700 Oe. Only the bottom six eigenvalues have been plotted with respect to the wavevector and these wavectors have been chosen in the z-direction.*

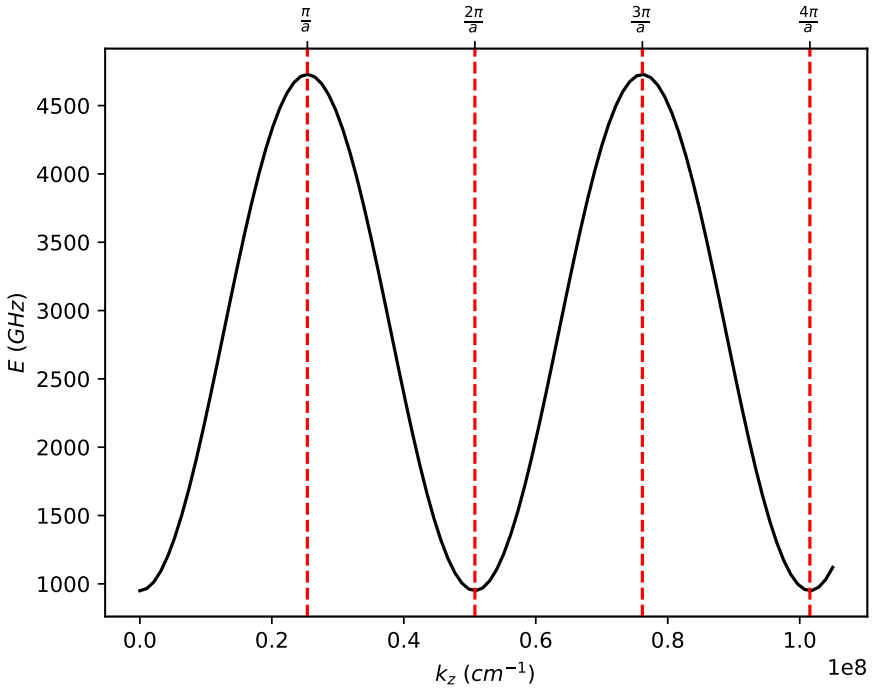

Figure 10: *Dispersion relation for a YIG film without holes. The lattice has one layer and the external magnetic field is 700 Oe. The wavevectors are in the z-direction. The boundaries of the first four Brillouin zones are indicated by the vertical red dashed lines. The boundary of the first Brillouin zone is at* $k_z \approx 2.5385 \cdot 10^7\ cm^{-1}$.

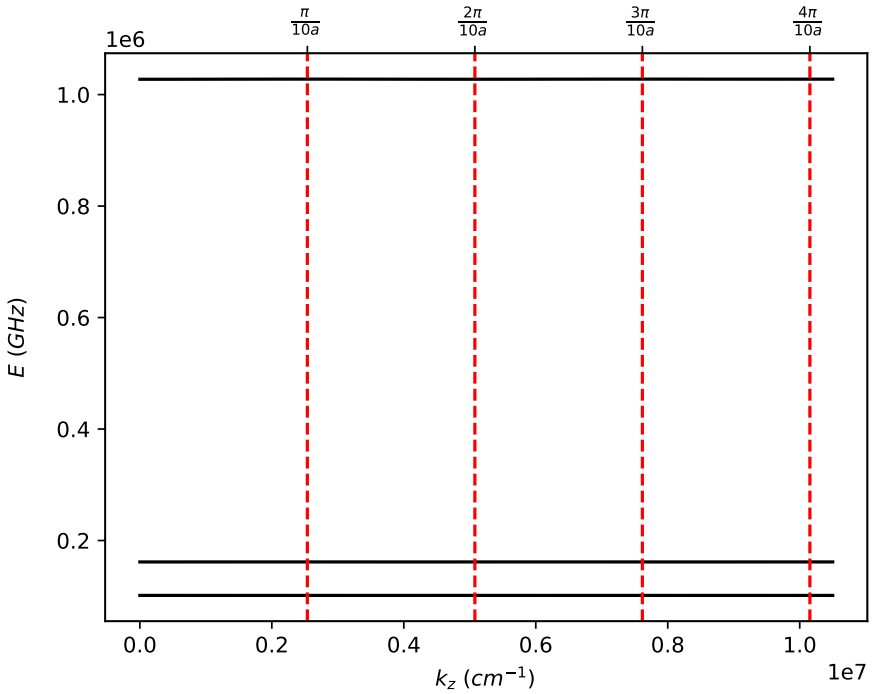

Figure 11: *Dispersion relation for a YIG film with holes. The lattice has 1 layer and the external magnetic field is 700 Oe. Here all three eigenstates are plotted with respect to the wavector which is in the z-direction. The boundaries of the first four Brillouin zones are indicated by the vertical red dashed lines. The boundary of the first Brillouin zone is at* $k_z \approx 2.5385 \cdot 10^6\ cm^{-1}$. *(Note the y-scale)*

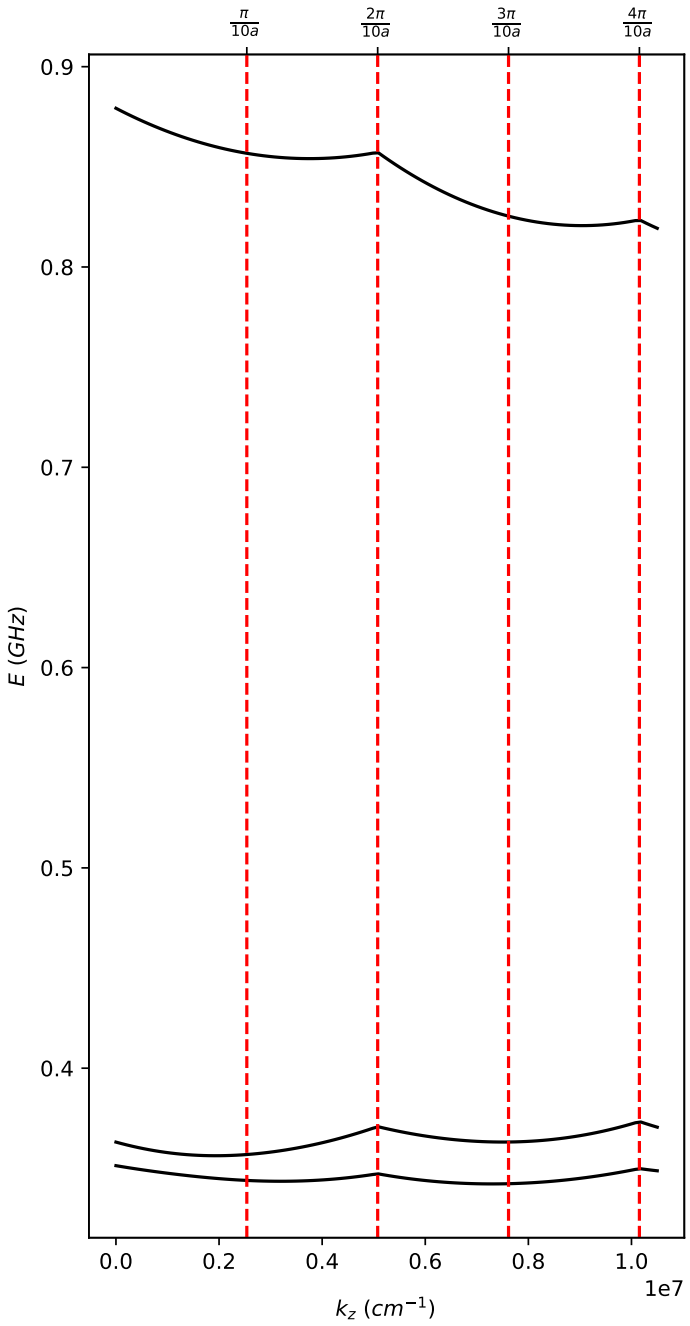

Figure 12: *Dispersion relation for a YIG film with holes, but with the exchange interaction neglected. The lattice has one layer and the external magnetic field is 700 Oe. Here all three eigenstates are plotted with respect to the wavevector which is in the z-direction. The boundaries of the first four Brillouin zones are indicated by the vertical red dashed lines. The boundary of the first Brillouin zone is at* $k_z \approx 2.5385 \cdot 10^6\ cm^{-1}$.

4 Discussion

In this chapter we will discuss the results of our research. In Chapter 3 we considered the effects of the Ewald summation and the dispersion relation, so we will discuss these subjects.

4.1 Comparison of the dipole terms

Let us start with our observations during the comparison of the dipole terms in Section 3.1 in the old case of a lattice without holes. As we have seen in Figures 5 and 6 there is hardly any difference between the explicit dipole term and the Ewald dipole term after a certain N. For small wavevectors as in Figure 5 we need at least $N = 2000$ and for large wavevectors as in Figure 6 we need at least $N = 600$. We conclude from this that the choice of using the Ewald summation or not, should not give different results in the dispersion relation, given the fact that we choose $N_{\text{Ewald}} = 10$ for the Ewald dipole terms and $N \geq 2000$ for the explicit dipole terms. As a result we chose to use the Ewald summation with $N = 10$. This means that we can choose our our lattice to be a 21 by 21 lattice, without getting different results than taking N larger than 2000. Due to this fact we need less computations which makes our simulations faster. This was also mentioned in Kreisel *et al.* [6]. Now for the new case of a lattice with holes we observed a similar behaviour. To get similar results for the explicit and ewald dipole terms we need an N of at least 2000 again. Now, however, we needed $N_{\text{Ewald}} = 20$ for the Ewald dipole terms. So now we choose our lattice to be 41 by 41. Remarkable is that the explicit dipole terms in the new case converge faster than the ones of the old case. An explanation lies in the fact that the sites are more seperated in the new lattice. If we assume that the lattices in the old and new case contain the same amount of sites, the lattice of the new case will take up more space due to the holes in it. As we said in Section 3.1.1 the explicit dipole term with a finite sum converges to the explicit dipole term with an infinite sum. The terms in the sum are the locations of the sites which are in general larger than in the previous case, so indeed we would expect the explicit dipole term to converge faster.

4.2 Dispersion relation

In Ref. [6] we can see the dispersion relation of a YIG film without holes. We followed the same theory and chose the same parameters and hence we got the same result which could be found in Figure 9. Instead of 400 layer we also plotted the dispersion relation for 1 layer in a non-logarithmic scale. In this case the boundary of the first Brillouin zone is at

$$\begin{aligned} k_z &= \frac{\pi}{a} \\ &\approx 2.5385 \cdot 10^7 \text{ cm}^{-1}. \end{aligned}$$

We expected a periodic behaviour, because our lattice is periodic and, indeed, we observe this. The reason we showed this, was because we found a similar behaviour in the dispersion relation for a YIG film with holes in it and where we neglected the exchange interaction. This could be found in Figure 12. What we expected to find was something similar as in Wang *et al* [7]. There the dispersion relation had a periodic behaviour and band gaps. In our dispersion relation we also see a periodic behaviour and band gaps, but the third dispersion branch has a slight decrease. Also around the boundaries of the Brillouin zones their dispersion relation has a maximum when we have a minimum and vise versa. Furthermore, the boundaries of the first two odd Brillouin zones are not precisely located at a minimum. As we have mentioned earlier we have neglected the exchange interaction in Figure 12. The reason was that the dispersion relation of a YIG film with holes as in Figure 11 has energies in the order of 10^6 GHz, which is much larger than what was the case in Figure 9 and in Wang *et al* [7]. Neglecting the exchange interaction circumvented this problem. A possible explanation could be that the exchange matrix as in equation (9) is wrongfully determined. Neglecting the exchange interaction can be justified, though, due to the fact that spin waves in the z-direction caused by the exchange interaction can not escape the holes.

5 Conclusion

In this chapter we will draw a conclusion of our research. Before that we give an overview of this thesis. Finally, we will give some ideas for future research.

5.1 Overview

Let us begin with an overview of our thesis. First we discussed the theory of our research. This included the Hamiltonians of the lattices in both the cases with and without holes. In particular we studied the dipole-dipole interaction and the use of the Ewald summation. Afterwards, we described how to find the dispersion relation of the Hamiltonians. What followed were our numerical results. We found that the dipole terms using the Ewald summation converged faster than the dipole terms without using the Ewald summation. Hereafter, we presented the results of our research in the form of dispersion relations. Finally, we discussed our results.

5.2 Conclusion of research

In our research we investigated the influence of holes in a YIG film. More precisely, we asked ourselves how the dispersion relation would change if there were holes. As we can see in Figure 11 we can now see band gaps, which were not there for the lattice without holes. The periodic behaviour is still there, but instead of the smooth shape like a sine function it now has sharp peaks. Also there are maxima instead of minima and vice-versa compared to what Wang *et al.* found. Note that we have neglected the exchange interaction here, because the energies are very large otherwise. We also have obtained side results. We have seen that we can use the Ewald summation for the dipole terms with a shift as in equation (11). We checked the validity of these dipole terms in Figures 7 and 8. In fact the dipole terms in these figures are approximations of the dipole term of the infinite lattice. We used the Fourier approximation which only holds for infinite periodic lattices. But provided that we took our lattice large enough these dipole terms should be excellent approximations. The dipole term using the Ewald summation converges fast which we used in our advantage by only using the Ewald dipole terms in our simulation.

5.3 Outlook

The largest problem in our research was the exchange energy creating high energies in our dispersion relation. Further theoretical and numerical research on this topic should be useful. Moreover we saw in Figure 12 that the third dispersion branch slowly decreases, while we expect it to be periodic. So also here more research should be useful. We wanted to investigate a lattice with holes as in Figure 3. What we could have changed, are the sizes of the strips compared to the holes. For example we suggest taking the width of the holes to be smaller than the width of the strip of sites. In this way we could obtain more insight into how the geometry of the YIG film influences the dispersion relation of the spin waves. What also could have been done, is adding a periodic array of spherical holes in our film. This has been investigated in Ref. [10] where they fill these holes with iron. They have predicted that there will propagate chiral spin wave edge modes along the boundary of the film which are the result of the topology of the crystal. Another interesting concept is the fact that we saw bandgaps. A questions that arises is how these bandgaps emerge, so further research on this is certainly possible. If there is a way to control the frequency of the spin waves using these bandgaps, it might be possible to use spin waves as a information carriers. There is, however, a limiting factor which is the spin wave damping [11]. This damping ensures that the decay lenth of the spin waves are in the order of tens of micrometer [12]. One could imagine it being very profitable to study spin wave damping. Other things we could have investigated were the angle and strength of the external magnetic field as in Ref. [6]. Changing the angle of the external magnetic fielded causes the dipole terms to change, because the direction of the spins will change. All these proposals for further investigations are to develop more ways to manipulate spin waves for the long term goal of using spintronics in electronic devices.

References

[1] Atsufumi Hirohata, Keisuke Yamada, Yoshinobu Nakatani, Ioan-Lucian Prejbeanu, Bernard Diény, Philipp Pirro, Burkard Hillebrands *Review on spintronics: Principles and device applications.* Journal of Magnetism and Magnetic Materials **509** 166711 (2020)

[2] Behin-Aein, B., Datta, D., Salahuddin, S. *et al. Proposal for an all-spin logic device with built-in memory.* Nature Nanotech **5**, 266–270 (2010)

[3] Ivan S. Maksymov, Mikhail Kostylev *Broadband stripline ferromagnetic resonance spectroscopy of ferromagneticfilms, multilayers and nanostructures* Physica E **69**, 253-293 (2015)

[4] M. A. Gilleo, S. Geller *Magnetic and Crystallographic Properties of Substituted Yttrium-Iron Garnet,* $3Y_2O_3 \cdot xM_2O_3 \cdot (5-x)Fe_2O_3$†. Phys. Rev. **110**, 73 (1958)

[5] A. V. Chumak, A. .A Serga and B. Hillebrands *Magnonic Crystals for Data Processing* J. Phys. D: Appl. Phys. **50** 244001 (2017)

[6] A. Kreisel, F. Sauli, L. Bartosch, P. Kopietz *Microscopic spin-wave theory for yttrium-iron garnet films.* Institut für Theoretische Physik, Universität Frankfurt, Max-von-Laue Strasse 1, 60438 Frankfurt, Germany. Eur. Phys. J. B **71,** 59–68 (2009)

[7] Z. K. Wang, V. L. Zhang, H. S. Lim, S. C. Ng, M. H. Kuok, , S. Jain, and A. O. Adeyeye *Observation of frequency band gaps in a one-dimensional nanostructured magnonic crystal.* Appl. Phys. Lett. **94**, 083112 (2009)

[8] D.I. Khomskii *Basic Aspects of the Quantum Theory of Solids: Order and Elementary Excitations.* Cambridge University Press, Cambridge, 2010.

[9] J. H. P. Colpa, *Diagonalization of the Quadratic Boson Hamiltonian.* Physica **93A**, (1978) 327-353

[10] Ryuichi Shindou, Ryo Matsumoto, Shuichi Murakami, Jun-ichiro Ohe *Topological chiral magnonic edge mode in a magnonic crystal.* Phys. Rev. B **87**, 174427 (2013)

[11] V. V. Kruglyak and A. N. Kuchko *Damping of spin waves in a real magnonic crystal.* J. Magn. Magn. Mater. **302-303** 272-276 (2004)

[12] L. J. Cornelissen, J. Liu, R. A. Duine, J. B. Youssef, B. J. van Wees *Long distance transport of magnon spin information in a magnetic insulator at room temperature.* Nature Physics **11**, 1022 (2015)